# How fast does a static charge decay? An updated review on a classical problem

Philippe Molinié

# How fast does a static charge decay? An updated review on a classical problem.

Philippe Molinié

Laboratoire de Génie Electrique et Electronique de Paris (GeePs), Université Paris-Saclay, CentraleSupélec, CNRS, Gif-sur-Yvette, 91192, France

philippe.molinie@centralesupelec.fr

**Abstract**

Understanding and modelling the static charge decay on an insulating material surface have been the topic of numerous research works since the nineteenth century. After an introduction on this historical context, a selection is presented here covering the various phenomena that may be held responsible for the decay: ion deposit from the surrounding atmosphere, charge injection and transport through the conduction and trapping levels of the solid, internal polarization by free carrier motion or dipole polarization, as well as surface conduction and migration of the deposited charge along the surface.

Surface potential measurements are a convenient technique to study these various types of charge motion but the underlying complexity concerning their interpretation is often neglected. Depending on the context, the law of electrostatics may produce a hyperbolic as well as an exponential decay. On an insulating polymer, or any other disordered insulator, charge transport is dispersive, and conduction as well as dipolar polarization responses are described by time power laws. The knowledge of this time response is not sufficient to build a convincing physical model, because of the universality of this response, which leaves many degrees of freedom to interpret the data. Knowledge of the possible elementary processes and their signatures in the observables is therefore requested before the implementation of curve-fitting procedures.

**Keywords**

Surface potential decay, electrostatic measurements, dispersive transport, surface conduction, charge trapping, electrets

## 1 Introduction

Electrostatic risk is an important issue in many sectors of modern life, due to the ubiquitous presence of strongly insulating materials. It is a vital concern in several industries [1] as for instance concerning spacecraft design and operation [2], or electronic circuits protection [3]. The control of static charge on insulator surfaces is also an issue for the development of the high voltage direct current (HVDC) systems required to connect networks with renewable energy sources at long distance [4–6]. Charge stability may on the opposite be sought to produce electrets [7,8] for various purposes, energy harvesting for instance [9], or to allow electrostatic charge separation for plastic waste treatment [10]. In these situations and many others, the question of charge decay on insulating materials is central. It has been the topic of many research works, both theoretical and experimental. As early as 1854, Kohlrausch reported [11] that the potential decay of charged Leyden jars did not follow the exponential law that could be foreseen assuming a leak proportional to the charge, but rather a "stretched exponential" $exp\left[-(t/\tau_0)^{\beta}\right]$. This observation was then largely forgotten, until it was rediscovered in 1970 by Williams and Watts [12]. The stretched exponential is nowadays in common use to model the dielectric response. This kind of behavior involving time power laws in dielectrics is indeed universal, as Jacques Curie demonstrated 135 years ago [13] by absorption current measurements (Curie-Von Schweidler [14] law). Later Gross [15,16], and de Oliveira Castro [17] computed the consequences of delayed dielectric relaxation on the voltage decay and return voltage on an insulator obeying Curie-Von Schweidler law, using the superposition principle.

The interest on this question was markedly renewed in the end of the 1960s, due to the research effort dedicated in this period to xerography. One important technical concern of the copying industry was to master charge transport through the photoconductive layer used to transform an optical image into an electrostatic image, able to attract toner particles for printing. A lot of research was undertaken to study charge mobility and trapping in amorphous selenium, the best material for this purpose. Charges time of flight was measured by recording the current response in closed circuit when applying to a polarized selenium layer a pulse of light through a semitransparent electrode. However, voltage measurements in open circuit after an initial charge deposit by corona discharge, followed by a short illumination ("xerographic discharge"), were closer to the industrial problem. A new field opened, leading to many models and a fast progress in the theoretical understanding of charge transport in dielectrics, often coming directly from industrial teams, from Xerox [18–22], IBM [23–25], or Kodak [26,27]. Researches were also undertaken to develop electrostatic measurement techniques. The first commercially available non contacting feedback voltmeters were developed in Rochester, capital of the imaging industry, by Vosteen, and later sold under the brand of Monroe Electronics.

The most important theoretical result of this blossoming research period was the theory of dispersive transport, associated to a 1975 founding paper by Scher (a Xerox researcher) and Montroll [20]. It was realized that even a moderate disorder in the material may lead to a strong dispersion in the charges transit time through the insulator, and the developments of this theory built a new theoretical frame for the charge transport studies, in which the trap distribution in energy is central. Dispersive transport was then included in potential decay models [28–30]. Independently, an experimental observation in 1967 by Japanese researchers [31] led also to many theoretical models in the following decades: polyethylene films charged at a moderate potential keep after a long decay time a larger voltage than a surface initially charged at a higher potential (Figure 5). Analyzing this "cross-over" phenomenon, they observed that the decay was slower when covering the surface by a conductive paint, and assumed that this nonlinear phenomenon was necessarily linked to charge injection from the surface into the polymer [32]. Electrostatic models were developed to account for charge injection, assuming field-depending mobility, or partial surface retention [33–38]. The surface trapping properties and their interaction with corona ions were investigated using voltage decay measurements [39–42], and models of decay due to surface conduction were also developed [43–45].

At the same period and later, research on electrets developed, exploiting the trapping capabilities of newly developed fluoropolymers [46,47]. On the opposite, static charge remained a nuisance in many contexts, requiring continuous research on charge decay, for instance for the development of HVDC cables [48] and substations bushing or insulators for which the influence of ionic currents in the gas may be the main cause for the decay [49,50]. Understanding charge buildup an decay on resistive surfaces is also a complex issue for industrial conveyors [51,52], while xerography remains today a lively research field, with a variety of new photoconductive materials replacing selenium [53]. Charge decay has also been investigated at the micro and nanoscale using techniques derived from the atomic force microscopy [54,55]. Finally, surface potential measurement has proven to be a convenient technique for insulating material characterization, providing information about charge transport and trapping [22,56–59].

However, since many different physical processes may lead to similar dynamics, fitting a theoretical curve with the measured decay is not sufficient. Several experiments have to be combined to get a precise understanding of the physical processes. One of the current problems is that the link is often forgotten between the decay models developed in various periods and the context for which these models were developed, concerning either material, field, or environment. Recently published works show a general tendency by researchers to deduce from the potential decay experiment some fundamental physical parameters of the material (as charge mobility, or trap levels distribution in energy) without even questioning the validity of the model they use. Therefore, we believe that the largest possible overview of the models developed up to now to account for charge decay, and a discussion on their respective application domains should be of interest for the community. Past reviews that we published in the past on this topic [60,61], need to be updated and completed. This article is devoted to this task.

## 2 Time constants that varies

IEC/TR 61340-1 standard [62] defines insulators, *"on which charge may have enough stability to be able to produce electrostatic effects"*, as structures with resistances above $10^{11}\ \Omega$. For instance, to be considered as insulating, the resistivity $\rho$ of a square plate of side $l = 10\ cm$ and thickness $d = 1cm$ has to be greater than $\rho = R\,l^2/d = 10^{13}\Omega.cm$. Assuming a relative permittivity $\varepsilon_r = 2$, the charge decay time constant for this material should then be higher than $\tau = \rho\varepsilon_r\varepsilon_0 = 1.77\ s$.

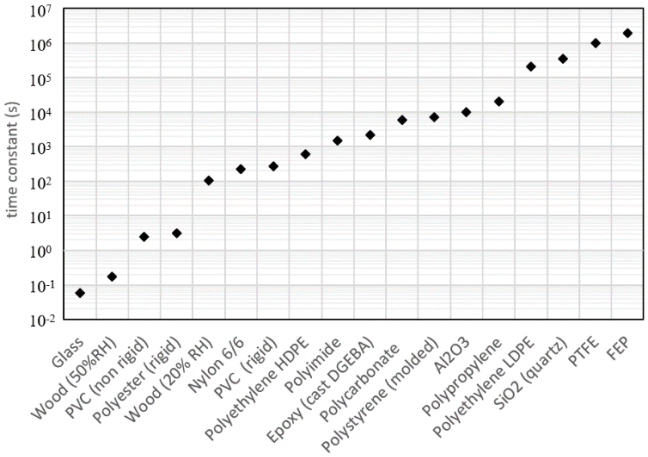


Figure 1 : Typical time constants computed from permittivity and ASTM D257 resistivity measurements for some common insulating materials. Data from [63] except glass from [64] and wood from [65]

Insulators according to this definition may present a wide spectrum of responses to the electric charge. Figure 1, we computed the charge stability for a set of usual insulating materials at ambient temperature and relative humidity, by multiplying the material permittivity by the typical material resistivity given in the literature. Resistivity values have been obtained using the ASTM D257 standard, which prescripts to realize the measurement 1min after applying the DC voltage to the insulator [66]. However, the assumption that a "time constant" exists implicitly assumes an exponential decay of the charge, i.e a resistance-capacitance model. Figure 2 presents experimental data of the potential decay (reduced to the initial charging value) with time, for two common electrical insulating materials. The red curve shows the exponential decay with the time constant that would be deduced from an ASTM measurement 1min after charging (2100s for epoxy, 4000s for XLPE). This time is supposed to be the time when the potential has decayed to *1/e* (36.8%) of its initial value. However the time really necessary to reach this potential is about 250 times higher in the first case (following an estimated trend curve), and 7.5 times higher in the second case.

Electrets, dedicated to obtain an almost infinite charge stability may present on the very long term an exponential behavior, as reported for instance in [7] for fluoroethylenepropylene electrets at 95°C. However, usual insulating materials with a charge stability from one minute to a few weeks usually follow the "universal" behavior made of time power laws, described by Curie and reviewed in details by Jonscher [67]. Examples concerning potential decay may be found for instance in [68] and [48] for low and high density polyethylene, in [69] for silicone and EPDM rubber SIR, in [70] for epoxy, and in [54] on PMMA. Resistivity and permittivity values given by textbooks are thus unsuitable tools to predict the charge decay. A correct model beyond the exponential behavior is an absolute necessity.

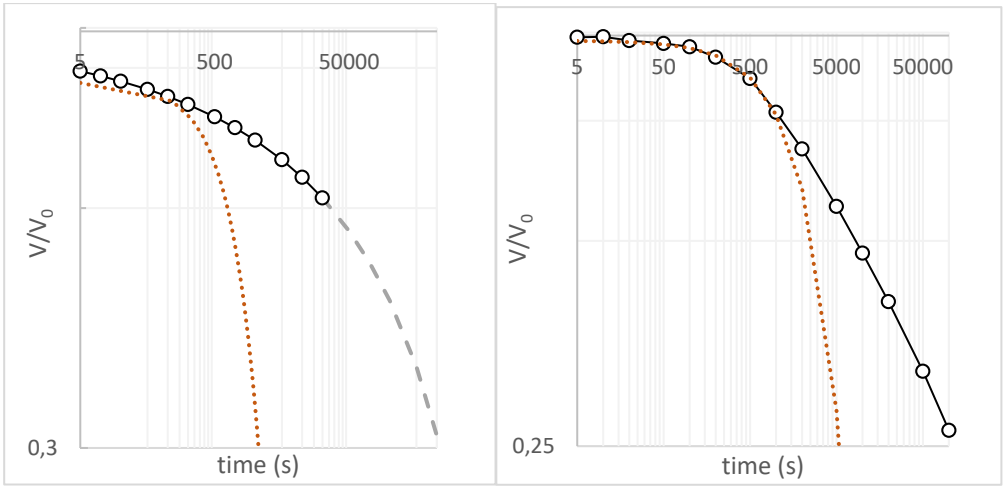


Figure 2 : Potential decay (log-log plot) on epoxy and XLPE using experimental data from [70] and [68] (black circles) compared to the exponential decay with a time constant measured 1 minute after charging (red dots)

## 3 Electrostatic influences and environment

The potential of a charged insulator depends on its environment, and a measurement device may influence it greatly. Figure 3a presents a charged surface element and the field lines connecting it to its environment, with a capacitive equivalent circuit. The surface potential may be deduced from measurements with a grounded field mill (Figure 3b), but the loss of potential due to the capacitance between the instrument and the surface has to be considered. On the opposite, using an electrostatic probe (Figure 3c), the field lines are prevented to flow between the insulator and the probe, thus reducing the total capacitance, and increasing the potential compared to the potential without probe [71].

The thickness of the insulator is of great importance in this sensitivity of the potential to its environment. For a thin grounded dielectric, the capacitance to its grounded side is usually much higher than the other capacitances involved in the potential determination, and the difference between the three cases described here may remain negligible. This situation changes however drastically for a charge distribution located far from the ground, whose potential depends on many external influences.

Besides, the influence of a measuring instrument may have an important influence on the dynamics of the potential decay, due to the atmospheric ions collection by the surface. When part of the field lines are flowing in the atmosphere from the charged surface, ions and charged particles of opposite polarity are attracted, following field lines, thus contributing to the potential decay, especially on a thick insulator surface, with a low capacitance to the ground. This is a common situation for HVDC insulators or bushings, on which charge buildup and dissipation has been widely studied [4–6,49,50]. In these studies, to avoid a large perturbation of the measured potential, it may be deduced from the measurements by a field mill at a large distance, or using an electrostatic probe and removing it as far as possible from the studied surface between

successive measurements. The system is thus assumed to follow an evolution close to its "natural" evolution. In this context, the decay may be mainly due to the ion drift current flowing to the charged surface.

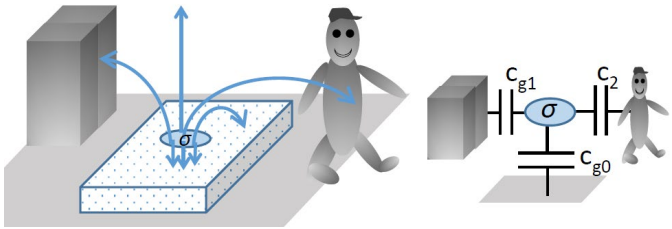


a. Without any measurement instrument

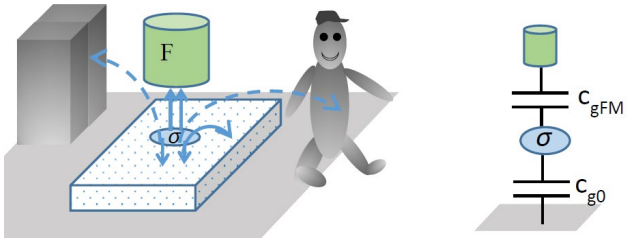


b. Influence of a grounded field mill

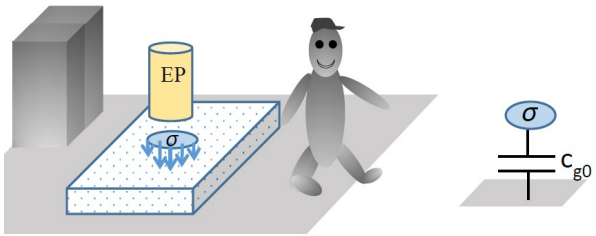


c. Influence of an electrostatic feedback potential probe

Figure 3 : Electrostatic field lines and influences on three different contexts.

The ion atmospheric density is highly variable. Production and recombination rates are both depending on the environment. A mean value of the ion generation rate due to radiation (cosmic rays and terrestrial radioactivity) is typically 10 $s^{-1}cm^{-3}$ [49] but it may increase, especially in underground installations, with radon gas accumulation, as underlined in [72]. Atmospheric ions may also be created by electronic impact when high electric fields are present. Concerning recombination, neutral or charged surfaces, ventilation and air filtration systems capture ions of one polarity or both; dust and aerosol particles may also act as recombination centers, or at least as gathering centers for ions of opposite polarities. Ion concentrations measured in a recent study [73] were in a range from 200 to 2000 ions.$cm^{-3}$ in typical indoor and outdoor atmospheres, between 100 and 500 ions.$cm^{-3}$ in clean rooms, while they were so low in a closed glovebox (below 10 ions per $cm^3$) that they could not be determined. It was also shown in this work that a charged PTFE insulator strongly reduces the ion density in its environment as far as 3 meters away, driving almost any charged species at a one meter distance.

A simple calculation may be useful to get a better understanding of this phenomenon, and compute its consequences on the potential decay. Assuming in the gas a positive ion density $n_+$, a negative ion density $n_-$, an ion generation rate $g$ and recombination rate $k_r$, at equilibrium without any applied electrostatic field:

$$g = k_r n_- n_+ \tag{1}$$

Assuming electroneutrality, at equilibrium:

$$n_- = n_+ = \sqrt{g/k_r} \tag{2}$$

The negative and positive ions current densities flowing to a charged surface obey the continuity equation:

$$\frac{1}{q}\vec{\nabla}.\overrightarrow{J_-} = -\frac{1}{q}\vec{\nabla}.\overrightarrow{J_+} = g - k_r n_- n_+ \tag{3}$$

Considering only conduction, neglecting diffusion and space charge effects:

$$\mu_{-}\vec{E}.\vec{\nabla}n_{-} = -\mu_{+}\vec{E}.\vec{\nabla}n_{+} = g - k_r n_{-} n_{+} \quad (4)$$

$\mu_+$ and $\mu_-$ being the positive and negative ions mobilities.

It is not possible to give an analytical solution of these coupled nonlinear equations. A detailed treatment of this problem may be found in [74]. We consider only here two asymptotical situations.

At low fields, if the ion generation is much higher than the conduction current, the equilibrium between generation and recombination is not affected by the field. Equation (2) is still valid and the gas acts as an ohmic resistance:

$$\vec{j}_{ohmic} \approx q\sqrt{g/k_r}\,(\mu_+ + \mu_-)\vec{E} \quad (5)$$

At high fields, the volume tends to be depleted, and charge lost by recombination tends to be negligible compared to charge collection by the surfaces:

$$\vec{\nabla}.\overrightarrow{J_-} = -\vec{\nabla}.\overrightarrow{J_+} = qg \quad (6)$$

At the collecting surface, assumed here to be a charged insulator, the flux of charges of the same polarity will be zero. At a large distance, the flux of charges of the opposite polarity may also be assumed to be zero. The total current density on the insulator surface (saturation current) is due to the flux of these charges arriving on the insulator, and may thus be evaluated by integrating the charge generated per unit time over a volume delimited by a tube made by the field lines arriving on the surface:

$$j_{sat} = \frac{1}{S}\iint_S \vec{j}d\vec{S} = \frac{1}{S}\iiint_{\mathcal{V}} \vec{\nabla}.\vec{j}dv = \frac{qg\mathcal{V}}{S} \quad (7)$$

The external limit of this volume may be considered as the transition of the high field region to the region where recombination predominates, preventing charges to migrate to the high field region. An order of magnitude of the field corresponding to this transition was evaluated in [49]. Considering two plane electrodes separated by $d = \mathcal{V}/S = 30cm$, with $g = 10.s^{-1}cm^{-3}$, $\mu_+ = \mu_- = 1.6\,cm^2V^{-1}s^{-1}$ and $k_r = 1.5\,10^{-6}\,cm^3s^{-1}$, saturation occurs for a field $E = 30\,Vm^{-1}$ with $j_{sat} \approx 4.5\,10^{-17}\,A.cm^{-2}$.

Concerning an insulator with thickness $d$ and relative permittivity $\varepsilon_r$ charged at $V$, the charge density per unit surface to be discharged is $\sigma = V\,\varepsilon_r\varepsilon_0/d$. Considering typical values $\varepsilon_r = 2, d = 1cm, V = 1000\,V$ the charge density to be discharged is $\sigma = 1.8\,10^{-10}C.cm^{-2}$. Assuming the neutralization current density deduced from the above model, the complete discharge time would be $4\,10^6 s$, more than 46 days, while a thinner 1mm film would lose its charge within 460 days. However, experiments on the natural decay of a charged insulator far from any perturbing measuring instrument report much shorter discharge times. In [50], the charge deposited on a charged 1cm thick epoxy sample decays within 400 min, corresponding to a loss of 20nC. On a mean surface estimated at 7 $cm^2$, the corresponding neutralization current density would be in this case 1.2 $10^{-13}$ $A.cm^{-2}$. In [75], a 3mm thick PTFE sample charged at 3kV loses 400pC.$cm^{-2}$ per hour, corresponding to a current 1,1 $10^{-13}$ $A.cm^{-2}$.

The reason for such a discrepancy lies in the field geometry. The field lines between plane electrodes are parallel, hence a small area on a given part of the electrode collects only the ions present in a field flux tube having a constant section. On the opposite, when a unique patch of charge is deposited on a given insulating surface, it collects the charge coming from a much larger volume, only limited by recombination at a distance where the field becomes weaker, or by the presence of another charged surface also attracting part of the field lines. In the plane to plane experiment with a distance 30cm, for a 1$cm^2$ surface this volume is reduced to 30$cm^3$, while considering the same surface draining the volume of a half sphere of radius 30 cm, it will be 4.24 $10^4$ $cm^3$ (1400 times higher), leading thus to a theoretical current of 6.4 $10^{-14}$ $A.cm^{-2}$. This effect is clearly visible on some experiments. For instance in [50], the presence of a charged epoxy sample in the vicinity of the test sample strongly limits the decay on the side of the charged epoxy. The key parameter to determine the amplitude of the decay on a point of the surface due to gas discharge is the associated volume in the surrounding space where field lines are coming to the insulating surface.

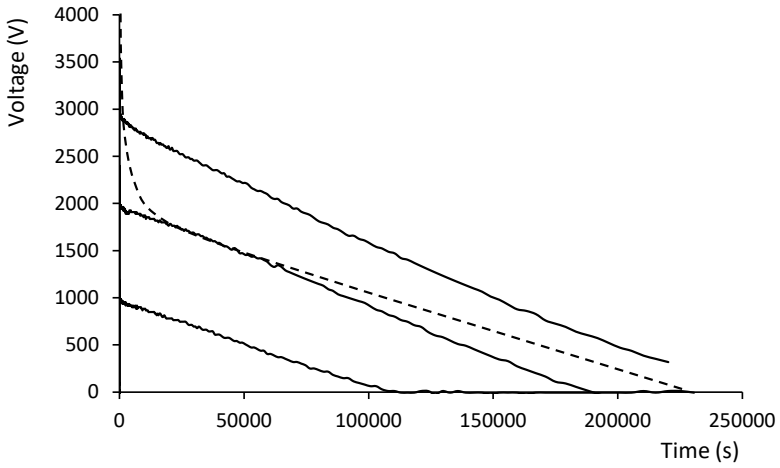


Figure 4: Potential decay of a charged levitating object for various initial voltages [76]

Concerning the time dependence of the voltage decay, the above model and observations imply that it is entirely depending on the generation rate, since the lifetime of the ions before recombination or collection by surfaces is short compared to the typical durations of the voltage decay experiments. Hence a constant charge generation in the collection volume implies a linear decrease of the voltage. This can be verified in cases where gaseous neutralization is the only cause of the potential decay. For this purpose experiments were performed using an electromagnetic levitation system [73,76]. Except at low fields in [73] where a time power law is observed, a linear decay is observed (Figure 4), with a slope (about 100V per day in [73] and 760 V per day in [76]) depending on the environment but independent from the surface voltage. Other experiments [77] on thick epoxy and Teflon insulators in SF6 also exhibit linear decays, with slopes which does not depend on the material. The authors rightly conclude that in practical gas-filled systems, the decay time of electrostatic charges on insulators will be inversely proportional to volume and pressure of the system, and that whenever, in addition to the charged insulator, conductors, charged at the same polarity, are present, the decay time of the surface charges is likely to increase. Another observation which is not intuitive, and would deserve a complete treatment, is that of hollows progressively dug in the center of the potential distribution on large insulators, observed for instance in [50] or [75]. They are attributed to the fact that field lines are more concentrated in the center of the distribution.

Concerning the influence of the measurement, operating a field mill may slightly reduce the volume to be gathered, hence reduce the ionic flux on the surface, while using an electrostatic probe entirely cancels the gas neutralization process. Continuous measurement with an electrostatic probe is the best way to minimize the effect of the environment, so it is best suited to characterize the insulating material properties, while to check the real charge density evolution of a system, measurements have to be discrete, with the instruments removed between the measurements.

## 4 External charge injection and transport

### *4.1 Simple electrostatic models*

Let us consider a grounded insulator with large lateral dimensions compared to its thickness $L$, so that the physical quantities only depend on the distance to the surface $x$. The external field is assumed to be zero (open circuit), and a charge has been injected at $t = 0$ into the insulator, with a given initial distribution in the vicinity of its surface, by a high illumination pulse on a corona charged surface, or by another kind of excitation. The surface potential at a given moment is:

$$V(t) = \frac{1}{\varepsilon}\int_0^L x\rho(x,t)dx \tag{8}$$

The deposited charge drifts into the volume, according to the laws of Electrostatics. The field seen by a charge located at $X = f(t)$ depends on the charge density integrated between this charge and the surface:

$$E(X) = \frac{1}{\varepsilon}\int_0^{f(t)} \rho(x)dx \tag{9}$$

Neglecting diffusion, the velocity of this charge will be an increasing function of the field, and therefore of its position in the distribution: the distribution may be seen as a succession of charge sheets moving at constant speed. The front of the distribution has a maximum speed, while the back, subjected to a zero field, remains fixed. Hence the charge distribution expands, charges being prevented to overtake one another if trapping is excluded. Assuming a constant mobility $\mu$ of the charges:

$$\frac{\partial}{\partial x}(\mu\rho E) + \frac{\partial \rho}{\partial t} = 0 \tag{10}$$

Integrating twice this continuity equation in $x$ and dividing by $\varepsilon$:

$$\mu \int_0^L \frac{\rho}{\varepsilon} E dx + \frac{\partial}{\partial t} \int_0^L E dx = 0 \tag{11}$$

$$\frac{\partial V}{\partial t} = -\frac{1}{2} \mu E^2(L) \tag{12}$$

Before the transit time the field at the counter electrode remains equal at the initial value: $E(L) = V_0/L$ $V_0$ being the initial potential (assuming the whole charge to be on the surface)

$$\frac{\partial V}{\partial t} = -\frac{\mu {V_0}^2}{2L} \tag{13}$$

The transit time is given by: $\tau = \frac{L}{\mu E(L)} = \frac{L^2}{\mu V_0}$ and $V(t) = V_0 - (V_0/2)(t/\tau)$ (14)

The potential decays following a straight line, whose slope is proportional to ${V_0}^2$ until the transit time of the front of the charge distribution, for which the potential has fallen to $V_0/2$. After the transit time, the amount of charge implied in the decay decreases with time. The charge density tends to be homogeneous in the insulator. Neglecting the changes in the shape of the distribution, both the density and velocity of the charge leaving the insulator are proportional to the mean remaining charge density, so that $\frac{\partial V(t)}{\partial t} \propto V^2$ which means that $V(t) \propto 1/t$. The decay tends asymptotically to be hyperbolic. From [23]:

$$\frac{\partial V}{\partial t} \approx -\frac{L^2}{2\mu} \frac{1}{t^2} \text{ and } V(t) \approx \frac{L^2}{2\mu} \frac{1}{t} \tag{15}$$

This calculation of the potential decay due to the charge drift under the influence of its own field in open circuit was published in a short annex of a paper written in 1968 by Kodak researchers (Reiser et al. [26]) and explained in more details by IBM researchers, Batra and Kanazawa [23]. Their work was completed by models developed by and with Wintle [24,33], to include diffusion and volume conductivity. A drift-diffusion model was also developed by Hill [36] stating that the concept of surface charge was oversimplified, because of the broadening of the charge distribution due to diffusion. However, very soon in the decay process, diffusion could usually be neglected due to the important field and quite moderate charge density gradients usually involved in insulators.

The interesting point about these quite simple electrostatic models, was that they suggest that recording the potential decay allows a determination of the charge mobility from the initial decay rate using equation (13). However the measurement of this quantity is not as easy as it seems. It has to be measured before the transit time of the distribution edge, but the injection process creating the initial charge distribution has also to be complete before the measurement. This may be done in xerography by using a very short and powerful light pulse, but it is generally not the case using a corona deposit. Moreover, even when with fast injection, the initial plateau predicted by these models for the potential derivative is almost never observed in non-crystalline insulators, including amorphous selenium. To account for the observations, several models were produced assuming a field-depending mobility [19,25,34]. However the main feature of the decay is a progressive decay during the experiment of the apparent charge mobility with *time* rather than with the *field* decrease. These electrostatic models were also not able to explain the cross-over of the curves (Figure 5) [34,78]. Other observations confirmed some predictions of these electrostatic models, as the proportionality of the decay with ${V_0}^2/L$ [79], but to explain the charge decay dynamics on insulating materials, trapping and detrapping processes have to be taken into account.

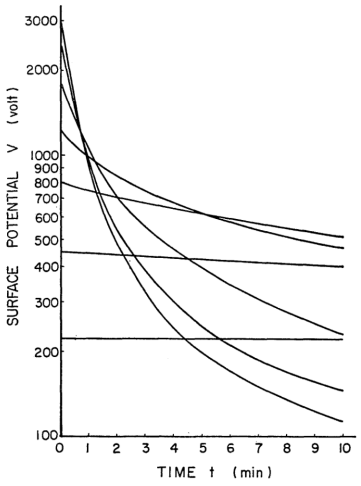


Figure 5 : Cross over of the potential curves on polyethylene films charged at various voltages [31]

*4.2 Surface charge retention*

Using electron beams, charge carriers may be directly injected into the volume electronic states, whereas classical charging techniques, by contact or corona, transfer charges, either ionic or electronic, in surface states. Depending on the material electronic affinity and work function, they are usually energetically lower than the volume transport levels. This has been

experimentally confirmed for instance by TSD measurements on polyethylene [40] showing that the deepest traps were on the surface, or by comparison of electron beam charging with corona on SiO2 [46] or with a charged electrode on polyimide [37]. With the exception of electron beam charging, injection of the deposited charge into the volume requires a given amount of energy. On most usual insulating materials, ambient thermal energy (1/40 eV) is too weak to inject a significant charge amount into the volume. The energy may be provided by photon activation (which is used to induce xerographic discharge) or by the activated particles deposited on the surface by the corona discharge. This corona activated injection (see Figure 6, where the surface is subjected after a given decay time to the exposure of neutral activated products of the corona discharge) has been studied quite intensively. First the effect of the photons accompanying the discharge was suspected [39] but it was proven later that the main effect was due to the neutral excited molecules [40], for instance by a transfer to the charge of the nitrogen oxide molecule vibrational energy [41]. This transfer is much more efficient in negative polarity, and it was assumed to intervene in the cross-over effect, since this effect, which had been observed by Ieda on 15µm polyethylene films charged with a corona discharge during several minutes at 3kV [31], also disappeared in some experiments when removing the excited molecules [40].

This progressive charge injection continues after the end of the charging phase, since it may be assumed that the corona activation creates a non-equilibrium distribution in energy of the charge carriers, as described in [57]. Surface traps with an energy close to the transport levels of the volume, which remain empty when the insulator is charged by contact, rubbing or by corona ions removing the excited molecules, get filled by an exposure to the corona discharge products, and may during the decay measurement be detrapped and drift into the volume. This is confirmed by the comparison with rubbing [42], and it has also been confirmed by TSD measurements that removing the excited molecules during charging leads to a more stable surface charge afterwards [40].

These observations form the physical basis of theoretical models assuming a progressive surface charge detrapping. In the model developed by Sonnonstine and Perlman [35], the motion of the initially injected space charge determines the first phase of the decay, then a surface emission regime is observed. At the highest charging fields, all the surface charges are injected instantaneously into the bulk and drift under their own fields to the back electrode. At intermediate fields, the charge injection is both field and time dependent, the time dependence being the stronger of the two processes. At lowest initial surface potentials, the charge injection is negligible and the surface potential may remain constant with time. Models assuming partial charge injection at high fields were shown to be the only possible way to account for the cross-over, and several of them were developed by other researchers [27,78]. Models assuming a double injection, both at the upper surface and from the back electrode have also been developed for long charging times at high fields [80,81].

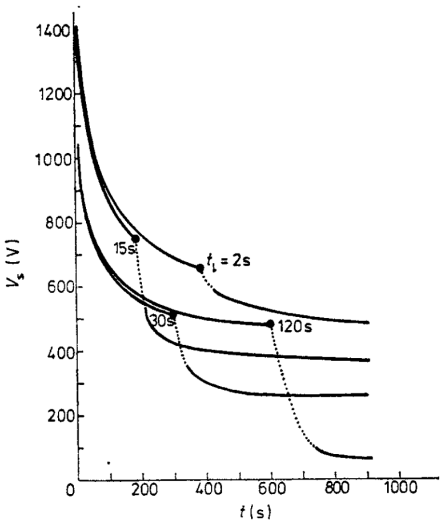


Figure 6 : Evidence of corona-assisted injection on a charged polyethylene film [39]

((●) corona exposure (removing ions))

### *4.3 Volume charge trapping and detrapping*

Considering surface traps only may be pertinent for thin insulators charged at high potentials. In this case, charge may be assumed to drift through conduction levels or shallow traps, but in the general case, for most high-resistivity materials, volume deep trapping plays a major role in charge transport. This question was of practical importance in xerography, where a residual potential always subsisted after the end of the xerographic discharge on amorphous selenium, which tended to increase after repeated charges and represented a major problem for the image quality [26,53]. Of particular importance was the determination of the product of the drift mobility of the charge carriers by their lifetime before trapping. Potential decay measurements allowed to derive this product from the ratio of the residual voltage to the initial applied voltage

[53,82]. Several models were published with electrostatic models of the voltage decay, including irreversible trapping at the scale of the experiment [26,83]. This kind of model gives a good account of the residual voltage, and may be well adapted to model a material where a well-defined mobility exists, due to a clear distinction between delocalized transport states, and localized trapping states. Mobility in the transport states may then also be computed at short times by the slope of the decay. However for most disordered materials, such clear distinction does not exist, and a continuum in the trapping distribution should be considered.

Charge motion is assumed to occur, either by multiple trapping/detrapping events (Figure 7), either by direct hopping between localized sites. In both cases the mobility in transport states is not a pertinent parameter to model the charge drift, since the decay is rather controlled by detrapping waiting times. At the beginning of the experiment, the insulator is in a non-equilibrium situation from an electrostatic and a thermodynamic point of view: charge is deposited at a given distance from the ground, and in electronic states which are not the lowest possible in energy. During the experiment, the charge drift reduces the mean distance of the charge distribution to the ground, while the repetitive capture/release process of the charge leads also to a reduction of their mean energy, burying them deeply in the trapping levels of the insulator.

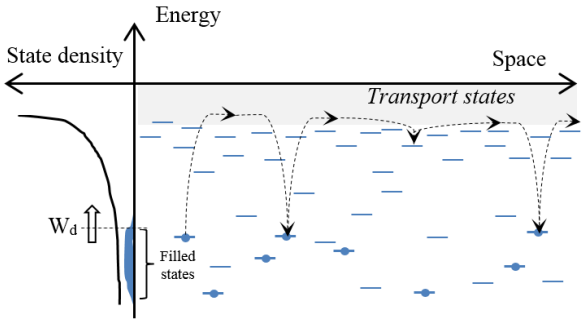


Figure 7 : Multiple trapping model of charge transport

This kind of motion in a trap distribution broadly dispersed in energy is named dispersive transport, a general concept introduced by Scher and Montroll in 1975 [20] and widely developed since [28,29,84]. Taking as a starting point a hopping model with broadly dispersed waiting times between hops (a process called Continuous Time Random Walk), dispersive transport is a general feature of disordered condensed matter. In this process, the distribution of the particle transit times, which are sums of random waiting times between successive hops, does not converge towards a Gaussian because of the weight in the distribution of rare events with long waiting times (due to deep trapping) as may be seen Figure 8. It follows another type of convergence, towards an “alpha-stable” Levy distribution. This kind of distribution tends to present an infinite value of its first moments (mean and variance). Hence parameters as mobility and mean time of flight of a particle through a given material cannot be defined. However this distribution of the transit times, and as a consequence concerning dielectrics the current decay during absorption current measurements (after applying a constant voltage) or the voltage decay after applying a pulse of charge on an insulator, present some characteristic features, as autosimilarity and time power laws [84].

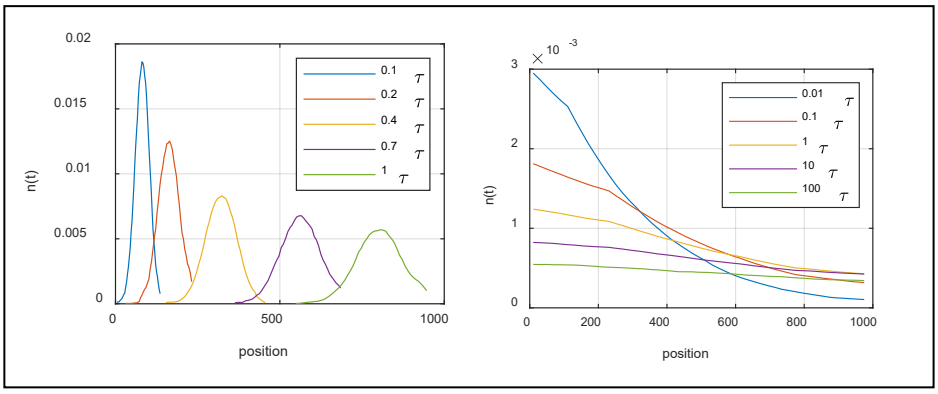


Figure 8 : Gaussian (left) and dispersive (right) charge transport (τ characteristic time)

The consequences of dispersive transport due to a broad trap dispersion for the potential decay experiment have been computed by Arkhipov and coworkers [30,85]. Taking at a starting point the calculation using successive sheets of charge, they introduced a continuous distribution of traps in energy and treated the problem using the concept of demarcation energy. The trapping probability for a trap located at a given energy $W$ below the transport energy levels where charge is assumed to be mobile (the “mobility edge”) depends on the trap density at this energy, while the release probability from this trapping level is inversely proportional to the exponential of its energy depth. The trapping level is at equilibrium when the trapping and release flows compensate. When a dynamical situation is considered, this equilibrium is reached first for the shallow traps, and then progressively for deeper traps. Considering the decay process over many time decades, at a

given moment, it may be assumed that the charge distribution is divided into two parts, the shallow traps in equilibrium with the transport levels, and the deep traps for which the release flow is lower than the trapping flow. The demarcation energy is the limit between these shallow and deep traps, evolving with time from a level close to the transport levels at the beginning of the experiment, towards much deeper levels after a long evolution.

Using this concept to simplify part of the calculation, and assuming an exponential decrease of the trap density with increasing energy distance from the transport levels, Arkhipov showed that the asymptotic behavior of the potential decay, at short and long times, follows time power laws, at least when part of the charge is kept trapped on surface levels. The trap density distribution being defined by:

$$n(W) = (N_t/W_0)e^{-W/W_0} \tag{16}$$

$N_t$ being the total trap density and $W_0$ the characteristic energy of the distribution. The calculation also considers the transit time $\tau$ of the distribution edge and a characteristic exponent $\alpha$ defined as:

$$\alpha = kT/W_0 \tag{17}$$

At short times, for $\ll \tau$ , $dV/dt$ is proportional to $t^{-1+\alpha}$, and to ${V_0}^2/L$ as it was in (13).

At long times, for $\gg \tau$ , $dV/dt$ is proportional to $t^{-1-\alpha}$ and to $L^2$ as it was in (15).

The transit time $\tau$ is shown here to be proportional to $(L^2/V_0)^{1/\alpha}$. For an identical initial $V/L$ field, it is not proportional to the insulator thickness as it was in the electrostatic model, but is proportional to $L^{1/\alpha}$, because of the increased probability of deep trapping events during the charge motion [85]. Another property of dispersive transport is autosimilarity (or "universality"): the shape of the potential derivative signal in reduced coordinates $log\left[\frac{dV/dt}{(dV/dt)_\tau}\right] = f(log[t/\tau])$ is independent of the applied voltage and sample thickness, as may be observed Figure 9 on low-density polyethylene, where $\alpha = 0.7$.

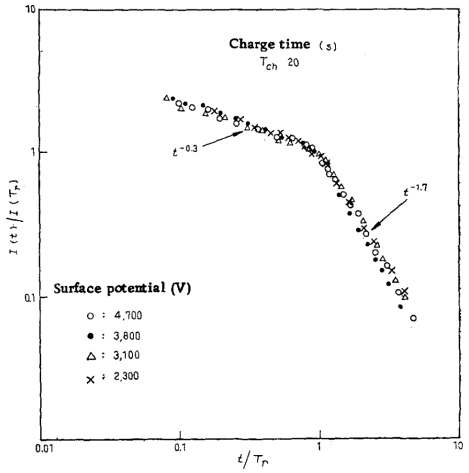


Figure 9 : Dispersive behavior of the surface potential decay on polyethylene films at various initial voltages [86]

The use of the demarcation energy in this model is a valid approximation for a broad distribution, when the transport is strongly dispersive ($\alpha \to 0$). However, for values of $\alpha$ above than 0.5, its validity has been questioned [84]. Other models have also been developed. In [87] a simplified model assumes an exponential trap distribution which leads to a stretched exponential for V whereas in [88] and [38] a time dependent mobility has been incorporated to account for the trapping in polyethylene.

The main parameter determining the charge transport in a disordered material is the trap energy distribution. This is still an object of many researches and discussions, and a recent and quite comprehensive review has been published by Teyssedre on this topic [89]. For a trap distribution with a low energy dispersion, a steady regime may be attained before the transit time. In this case, charge transport is not dispersive, but Gaussian and the use of an electrostatic model with a trap-controlled equivalent mobility may be pertinent [78]. For a broader distribution, the transport tends to be dispersive. This does not depend however from the trap distribution only, since, for the same material, increasing the temperature or the thickness may lead to a transition from dispersive to Gaussian transport [90].

On the opposite, for thin insulators subjected to high fields, the dynamics of the decay may be directly determined by the trap energy distribution, rather than by any spatial parameter. In this case, it is assumed that the transit time after charge detrapping is negligible compared to their residence time in traps in the time scale of the experiment. That means therefore that deep retrapping is neglected. If these simplifying assumptions are valid, the charge decay at a given time is only due to the emission of the traps located in the vicinity of the demarcation energy.

The characteristic time to release by thermal energy $kT$ a charge from a trapping level at an energy $W$ below the energy of the transport levels is $\nu^{-1}e^{-W/kT}$, $\nu$ being a characteristic attempt-to-escape frequency. The demarcation energy at time $t$ is then given by:

$$W_d = kT\ln(\nu t) \tag{18}$$

The detrapping current at $t$ is directly linked to the trap density distribution:

$$I(t) \propto N(W_d)\, dW_d/dt = \nu^{-1} N(W_d)\, kT/t \tag{19}$$

$N(W_d)$ being the density of filled states at the demarcation energy

Hence in this situation a direct image of the density of states may be obtained by plotting $tI(t) = f\big(kT\ln(\nu t)\big)$. This treatment has first been done by Simmons and Tam [91] using the isothermal absorption current. This method was then adapted by Watson [21,22] to the potential decay. By representing $t\, dV/dt = f(\log t)$, the shape of the trap distribution could be obtained. To determine the unknown frequency $\nu$, several experiments at different temperatures may be used, as illustrated Figure 10. Watson compared the results obtained by his method on 3.3 µm thick polystyrene films with a simulation of multiple trapping transport and shows a good correlation [22].

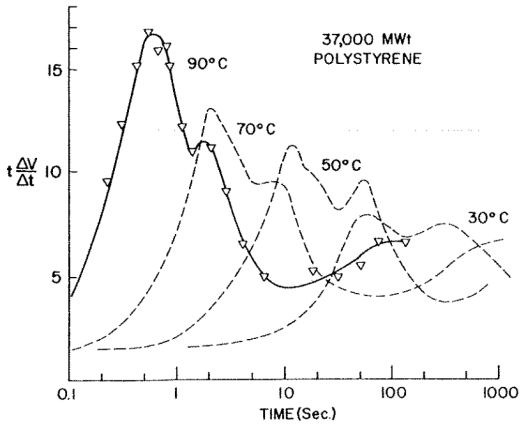


Figure 10 : $t\, dV/dt = f(\log t)$ plot for polystyrene at various temperatures [21]

This method is nowadays popular and is found in many publications determining directly the trap distribution from the potential decay, for instance in polyethylene [68], EPDM and SIR [69], epoxy [4], or ceramics [58]. However the founding assumptions for the validity of the model are usually forgotten by the authors, who erroneously apply this direct determination method of the trap energy distribution at moderate fields, or for thick insulators, unaware that in this case a multiple trapping and detrapping model has to be mobilized. The possibility to deduce the trap distribution using such a model is then another question, more difficult. Several authors doubt of this possibility [92]. Moreover, as has been remarked by Sibatov [84], as soon as a dispersive transport is involved with multiple trapping-detrapping events, the charge propagation features – and here, the shape of the potential decay - are determined by statistical laws, due to the fact that the trap distribution is broad in energy, rather than by a particular shape of this distribution.

As a conclusion, we strongly insist on the fact that the direct determination of the trap distribution in energy from the potential decay data is only possible on thin insulating films charged at high fields. However the $t\, dV/dt = f(\log t)$ representation remains useful in any case, since it provides a good representation of the decay dynamics that allows to separate different successive physical processes involved in the decay, as we demonstrated in [57]. In this paper one of the observed peaks, on thin polypropylene films at high fields, is attributed to progressive surface detrapping and in this particular case we estimated that it could provide a direct image of the surface trap density.

## 5 Internal free charge motion

In the preceding sections, we assumed that the insulator was entirely devoid of any intrinsic response, mobile charges being brought into the material (or on its surface) from the outside only. However, especially at low fields, the dominant mechanism leading to voltage decay is most often a slow polarization of the material under the influence of the applied field. We will examine in the next section the dipolar component of this polarization. Here we analyze the consequences of the presence of mobile internal charges in the material. Assuming the insulator to be in thermodynamical equilibrium, a given charge density of free charges carriers (electron, holes or ions) exists due to thermal activation, following the Fermi-Dirac statistics. Applying a moderate electric field, it may be considered that this distribution is unaltered. In this case (and in this case only), the material is characterized by a volume conductivity $\sigma_v$ proportional to the product of the density of the free charge carriers $n_i$ by their mobility $\mu_i$:

$$\vec{j} = \sigma\vec{E} \text{ with } \sigma_v = q\sum_i \mu_i n_i \quad (20)$$

$q$ being the elementary charge

Assuming a charge density $\rho$ in the volume of the material, the continuity equation may be considered:

$$\nabla.\vec{j} + \frac{\partial\rho}{dt} = 0 \quad (21)$$

For a constant conductivity, and considering the material permittivity $\varepsilon$, the Poisson equation implies that:

$$\nabla.\vec{j} = \sigma_v \nabla.\vec{E} = \sigma_v/\varepsilon\ \rho \quad (22)$$

The solution of (21) is then:

$$\rho(t) = \rho(0)e^{-t/\tau} \text{ with } \tau = \varepsilon/\sigma_v \quad (23)$$

A charge deposited anywhere in a material with a given resistivity, or on its surface, decays with a characteristic relaxation time equal to the product of its volume resistivity $1/\sigma_v$ by its permittivity. However, as has been underlined in the introduction, this "ohmic" behavior producing an exponential decay is usually not encountered on the materials with insulating properties making them suitable to induce an electrostatic risk. A field dependent conductivity may be assumed to account for the nonexponential shape of the decay as has been done in [93], assuming some kind of Poole-Frenkel field assisted detrapping. The gradual slowdown of the decay during the experiment may indeed appear as a consequence of the field decrease. However, as we have seen, this slowdown with time is usually mainly due to charge progressive trapping. To determine an eventual conductivity field dependence, experiments with several values of the initial potential cannot be avoided. Another mechanism implying internal conductivity may however explain the shape of the decay, which is assumed to be the main responsible for the dark decay of the surface voltage on amorphous selenium: the "xerographic depletion discharge". Here the free carrier density at thermal equilibrium is assumed to be negligible, but if a sufficient field is applied, charge carriers are assumed to be progressively detrapped, first from energetically shallow traps, then from deeper traps. This detrapping of carrier of a predominant sign leaves a remaining space charge of the opposite polarity [53].

The mechanism of the depletion discharge is the following [53]: the progressive, uniform, depletion in the insulator increases until the depleted space charge equals the surface charge. At this moment, called the depletion time $t_d$, the field is reduced to zero at the back electrode opposite to the surface charge. After $t_d$, the insulator will be separated in two regions. The region located on the side of the surface is defined by an integrated volume charge density compensating exactly the surface charge density. In this zone, depletion will continue to increase, hence its thickness will progressively decrease, leaving behind an expanding second region in which the field is null or slightly inverted, so that this region will slowly recover its space charge neutrality. The dark discharge exhibit different behaviors before and after the depletion time $t_d$. Considering an exponential distribution of the traps, the shape of the potential decay derivative exhibits the classical behavior of two asymptotic decreasing slopes with a sum equal to -1. In this model the potential at $t_d$ should be half of the initial potential [53]. This model may be considered as a negative image of the charge injection model.

This kind of model has been developed in [94], assuming a Poole Frenkel field assisted detrapping mechanism and an exponential trap distribution. The simplest picture is one in which free charge carriers are thermally generated in the bulk at constant rate and swept out rapidly compared with the generation rate. Using a broad distribution of the traps, this will also lead to a decay following two slopes [53]. The superimposed effect of injection from the surface may be added, via a surface charge generation rate. In [29] surface charge injection followed by multiple trapping transport in the volume is compared with homogeneous thermal generation of the charge carriers in the volume. Assuming the same trap distribution, both cases lead to the same power laws for the decay at long times. However their dependences with voltage and thickness before and after transit time are inversed (see Table 1). To distinguish them, a series of measurements at different charging voltages and samples thicknesses are thus required.

## 6 Dielectric absorption

Various physical phenomena may induce slow dipolar polarization in the insulators. An internal charge of both polarities may be trapped on some sites on polymer chains, and slow chain motion may occur under the influence of the applied field. On polycrystalline ceramics or polymers, composites, resistivity heterogeneity induces Maxwell-Wagner polarization, with a dynamics often falling in the time range of surface potential decay measurements. For this reason, even non polar material may exhibit a strong dipolar polarization response. Several studies have shown on common insulating materials the predominance of this response [95,96,70]. However, while this component of the insulator response to the field is central concerning dielectric spectroscopy, it is often neglected in the interpretation of surface potential data. The existence of these slow polarization processes will nevertheless induces a progressive decay of the potential, which in principle will tend towards an asymptotic non-zero value. It may be viewed as the consequence of a progressive increase of the insulator capacitance, the deposited charge being progressively screened, at least partly, by polarization charges.

In the frequency domain, dielectric spectroscopy data are commonly fitted using the phenomenological relaxation models of Cole-Cole [97], Havriliak-Negami [98] or Kohlrausch-Williams-Watts [12]. In the time domain, the dielectric response involves time power laws, concerning as well the decrease in the absorption current after the application of a DC voltage than the potential decay after a surface charge deposit. To describe the complete dynamics of relaxation, at least two exponents are usually necessary, an exponent lower than one at short times, and another larger than one at long times [67]. A correct mathematical treatment of this problem requires the calculation of the inverse Laplace transform of the transfer functions describing the spectroscopic data.

The theory of the consequences of this "dielectric absorption" concerning the voltage decay and "after effects" on capacitors, has been developed by ancient pioneering works by Gross [15,16] and De Oliveira Castro [17], mainly written in German, and almost forgotten today, with the exception of a recent paper by Mainardi [99]. We developed their ideas and provide an overview of this question in a recent paper, using also modern software to compute the shape of the potential decay due to this absorption phenomenon [100].

Let us consider a plane dielectric devoid of any conductivity with its lower side grounded. A brief charge deposit at *t=0* is assumed to charge instantaneously the insulator upper surface at a potential $V_0$. The existence of non-instantaneous polarization processes leads to a potential decay after charging that could be written as follows:

$$\frac{dV(t)}{dt} = \Delta V \phi_*(t) \qquad \text{with } \Delta V = V_0 \left(\frac{\varepsilon_\infty}{\varepsilon_s} - 1\right) \tag{24}$$

$\varepsilon_\infty$ being the material permittivity including the polarization phenomena fast enough to follow the electric field variations at the measurement scale, and $\varepsilon_s$ the static permittivity including the fast and slow polarization processes. $\phi_*(t)$ is the material dielectric response function to a step of charge [100]. There is a mathematical relationship linking this dielectric response, describing the potential decay (open circuit) in the time domain, with the frequency response deduced from dielectric spectroscopy measurements (obtained by current measurements in closed circuit). The Laplace transform of $\phi_*$ may be deduced from the frequency response $\tilde{\phi}(s)$ :

$$\widetilde{\phi_*}(s) = \frac{\varepsilon_s \tilde{\phi}(s)}{\varepsilon_\infty + (\varepsilon_s - \varepsilon_\infty)\tilde{\phi}(s)} \tag{25}$$

The polarization relaxation rate may be assumed to be proportional to its deviation from equilibrium (Debye relaxation):

$$\tilde{\phi}_D(s) = (1 + s\tau)^{-1} \tag{26}$$

and

$$\phi_*(t) = (1/\tau_1) e^{-t/\tau_1} \text{ with } \tau_1 = \tau \left(\frac{\varepsilon_\infty}{\varepsilon_s}\right) \tag{27}$$

In this particular case, the potential decay due to the polarization process is exponential. But as mentioned earlier this is quite exceptional on insulators. The usual frequency response involves a power law. For instance, a Cole-Cole behavior is described by the empirical relationship:

$$\tilde{\phi}_{CC}(s) = (1 + s^\alpha \tau^\alpha)^{-1} \qquad \text{with } 0 \le \alpha \le 1 \tag{28}$$

In this case, it has been shown [100] that the potential decay after charging follows a Mittag-Leffler function:

$$V(t) = V_0 - \Delta V \left[1 - E_{\alpha,1}(-(t/\tau_1)^\alpha)\right] \tag{29}$$

$$\frac{dV(t)}{dt} = -\frac{\Delta V}{\tau_1} (t/\tau_1)^{\alpha-1} E_{\alpha,\alpha}(-(t/\tau_1)^\alpha) \qquad \text{with } \tau_1 = \tau \left(\frac{\varepsilon_\infty}{\varepsilon_s}\right)^{1/\alpha} \tag{30}$$

The generalized two-variable Mittag-Leffler functions $E_{\alpha,\beta}(z)$ are special functions [101] among which the exponential is a particular case for $\alpha = \beta = 1$. The potential decay depends on $\tau_1$ (characteristic time), $\Delta V/V_0 = (1 - \varepsilon_\infty/\varepsilon_s)$ (slow polarization relative amplitude), and $\alpha$ (shape factor). A computation of three Mittag Leffler functions may be seen in dotted lines Figure 12 with different values of these three parameters.

The time derivative of the potential is decaying as $(t/\tau_1)^{1-\alpha}$ for $t/\tau_1 \ll 1$ and as $(t/\tau_1)^{-1-\alpha}$ for $t/\tau_1 \gg 1$.

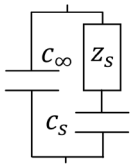

Figure 11 : Equivalent circuit for a Cole-Cole relaxation

A material following the Cole-Cole dielectric behavior may be modelled by the circuit given Figure 11. Lowercase $c$ and $z$ notations correspond to capacitance and impedance per unit area. The dipole $z_s$ complex impedance is $\widetilde{z_s} = \tau^{\alpha} s^{\alpha-1}/c_s$. It is a constant phase element (CPE): the ratio between its imaginary and real parts does not depend on frequency [97].

On several time decades, the response of an insulator is rarely depending on a single physical phenomenon. It may be seen as the sum of several elementary Cole-Cole relaxation processes in series, each described by equation (30) with its own parameters $\alpha_i, \tau_i$ and $\Delta V_i$, as shown Figure 12. [100].

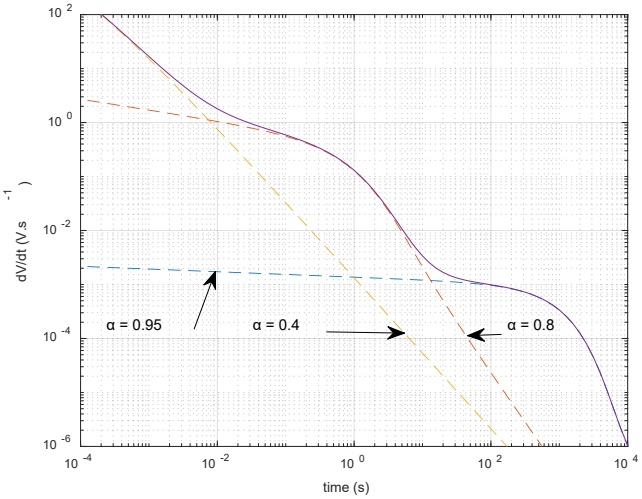


Figure 12 : Voltage decay due to three Cole Cole relaxation processes [100]

This description of potential decay due to Cole-Cole dielectric relaxation process may be extended to other classical types of relaxations (Kohlrausch-Williams-Watts, Havriliak-Negami) but to our knowledge the calculation of the potential decay has not been done and these descriptions do not allow to use simple equivalent circuits as given Figure 11 .

The physical interpretation of the power laws involved in the dielectric response has been largely discussed in the past [102]. It may be treated as a superposition of exponential relaxation processes with different characteristic times [103]. However as it has been remarked concerning the potential decay due to dispersive transport, this emergence of time power laws seems largely independent of the material specific features and a particular distribution of the relaxation times (DRT) could not be invoked as an explanation. The striking similitude between the signal produced by dielectric relaxation and dispersive transport also suggest a common origin of this time dependence.

## 7 Surface conduction

### *7.1 Introduction*

A large research effort has been devoted to the understanding and modelling of surface currents, caused either by surface conductivity or by charge injection from the electrodes. These currents have been suspected to be responsible for at least part of the absorption currents measured in polymers after the application of a DC voltage between electrodes, since several authors had remarked a dependence of the current with the electrodes perimeter [104–106]. These observations and explanations were later questioned but they provoked some interesting theoretical work on currents due to surface charge injection [107,108]. This question has also been – and still is - the focus of many researches in the field of HVDC devices development since surface conduction often determines the potential repartition along the DC insulators surfaces [44,109–113]. However, modelling surface lateral migration and conduction is from the electrostatic point of view more complex than volume conduction, since a 1D model cannot account for the phenomena: the depolarization of the insulator volume is always accompanying the potential decay due to surface conduction. Another question is the notion of surface itself since a gradient in physicochemical properties is always present. However in most practical situations in Electrostatics the surface may be seen as a 2D system. Assuming a 3D resistive surface layer of thickness $\delta$ and mean volume conductivity $\sigma_V$, its surface conductivity will result in the integration of its conductivity over the layer thickness ($\sigma_S = \delta\sigma_V$).

*7.2 Ohmic surface conduction*

Somerville [114] gave a detailed calculation of the charge spreading and potential decay due to ohmic surface conduction on an infinite resistive plane separating two dielectric half spaces, for instance air and a perfect insulator, the only boundary condition being a zero potential at the infinite. He remarked that the potential, fields and charge distribution in one of the half spaces at an instant $t$ after the charge deposit may be obtained by using the formula giving the same quantity at the same place at the moment of the charge deposit, and simply replacing the distance to the plane $z$ by $z + ut$, with $u = 1/2R\varepsilon_{eff}$ ($R$ being the plane surface resistivity and the effective permittivity $\varepsilon_{eff}$ the mean value of the permittivities of the two dielectric half spaces). In cylindrical coordinates, for a point charge $Q$ deposited at *t=0* on $(r = 0, z = 0)$:

$$V(r,z,t) = \frac{Q}{4\pi\varepsilon_{eff}(r^2+(z+ut)^2)^{1/2}} \tag{31}$$

On the center of the surface charge distribution:

$$V(0,0,t) = \frac{Q}{4\pi\varepsilon_{eff}\, u\, t} \tag{32}$$

In this oversimplified presentation of the model, the initial voltage is not defined at $t = 0$, but the interesting prediction of (32) is that the potential should in the long run decay hyperbolically with time. Wintle [55] used for instance this model to compute the surface spreading of a patch of charge deposited by an AFM due to surface conduction.

This kind of modelling is adapted when the sample thickness is large compared to the width of the charged area.When however the effect of the ground electrode beneath the sample has to be taken into account, the calculation is different. An elementary two dimensional model may establish what should be the final shape of the charge distribution and the time constant of the decay. Let us consider an insulator of width $L$, thickness $d$ and permittivity $\varepsilon$, with a surface conductivity $\sigma_s$ and a surface charge density $\sigma(x,t)$. Assuming the field lines to be approximately vertical and directed towards the back electrode only, the surface potential is proportional to the charge density:

$$V(x,t) = d\sigma(x,t)/\varepsilon \tag{33}$$

According to the continuity equation:

$$\frac{\partial V}{\partial t} = \frac{d}{\varepsilon}\frac{\partial \sigma}{\partial t} = -\frac{d\sigma_s}{\varepsilon}\frac{\partial E_x}{\partial x} = \frac{d\sigma_s}{\varepsilon}\frac{\partial^2 V}{\partial x^2} \tag{34}$$

This is a classical heat equation. A stable distribution shape is obtained if $V$ could be written: $V = V_0 f(t) g(x)$

$$\frac{1}{f(t)}\frac{\partial f(t)}{\partial t} = \frac{d\sigma_s}{\varepsilon}\frac{1}{g(x)}\frac{\partial^2 g(x)}{\partial x^2} = -\frac{1}{\tau_s} \tag{35}$$

The decay tends towards an decreasing exponential $(t) = e^{-t/\tau_s}$ . The spatial dependence of the potential is defined by:

$$g + \frac{\sigma_s \tau_s d}{\varepsilon}\frac{\partial^2 g}{\partial x^2} = 0 \tag{36}$$

$$g(x) = \cos kx \;\text{ with } k = \sqrt{\frac{\varepsilon}{\sigma_s \tau_s d}} \tag{37}$$

The potential should be zero for $x = \pm L/2$, thus $k = \pi/L$ and:

$$\tau_s = \frac{\varepsilon}{\sigma_s d k^2} = \frac{\varepsilon L^2}{\sigma_s d \pi^2} \tag{38}$$

$$V = V_0 e^{-t/\tau_s} \cos(\pi x/L) \tag{39}$$

This simple calculation (considering the insulator as a distributed RC transmission line) suggests that, whatever the initial charge distribution shape, the final shape of the charge distribution due to the surface condition tends towards a cosine, with a characteristic relaxation time given by (38).

Crisci et al. [112] published a more sophisticated computation of the surface potential decay due to combined volume and surface ohmic conduction, but their conclusions were identical. They showed that: *"the first part of the decrease with time of the surface potential is strongly influenced by the initial distribution of charges and cannot be used to determine the surface conductivity. On the other hand, at rather long times after the surface has been charged, the potential of the surface follows an exponential variation with time…"*. The time constant $\tau$ of this asymptotical exponential decay is determined by a combination of the volume and surface conduction ($1/\tau = 1/\tau_v + 1/\tau_s$), $\tau_v = \varepsilon/\sigma_v$ being the classical relaxation time while the time constant related to surface conduction depends on the geometry. For a 2D problem in Cartesian coordinates, Crisci finds (38). Assuming a cylindrical symmetry, the relaxation time due to surface conductivity is slightly different:

$$\tau_s = \frac{R^2\varepsilon}{\mu_1^2 \sigma_s d}\text{ , } \mu_1 \approx 2.41 \text{ being the zero of first order of the Bessel function } J_0 \tag{40}$$

Robinson[51] analyzed the practical situation of a charged resistive web suspended between two conveyance rollers. No volume conductivity is involved, but two grounded surfaces were considered on both sides of the web. Noting their distances $g$ and $d$ while assuming permittivities $\varepsilon_1$ on one side and $\varepsilon_2$ on the other side, Robinson obtains:

$$\tau_S = \frac{L}{\pi\sigma_S}\left[\frac{\varepsilon_1}{\tanh(\pi g/L)} + \frac{\varepsilon_2}{\tanh(\pi d/L)}\right] \tag{41}$$

For a small value of $d/L$, the expression is reduced to the value found above (38) and in [112].

The important result to be kept in mind is that the charge relaxation time due to surface conduction processes is not an intrinsic property of the material with a given surface conductivity. It increases as the distance to the grounded plane decreases. Charge relaxation is slowed because for the surface current is proportional to the tangential electric field which becomes smaller, for a given charge density, as the distance to the grounded plane decreases. Another important difference between surface and volume conductivity is that charge relaxation due to a homogeneous volume conductivity will not lead to the spread of the space charge: it will vanish, due to the screening effect, according to equation (23). On the opposite, surface conductivity will lead to charge spreading until the cosine shape of the surface charge is attained. Simulations [112,115] clearly show this effect. It is then possible to detect surface conduction by measuring the initial potential buildup in the vicinity of the initial charge distribution due to the broadening of a sharp initial distribution [112].

Using also a distributed RC transmission line model, Haenen [116] computed surface charging of a resistive surface from side electrodes, and the following decay. Wintle [111] considered the case of a resistive surface between electrodes, but without any ground electrode, and deduces an asymptotic exponential decay, rather than the hyperbolic decay computed for a bare surface.

To account for the threshold effect observed in the potential decay for electrets stored at various humidity levels, percolation models have also been developed [117]. The main hypothesis of this kind of model is that ambient moisture induces growing conductive patches around condensation nuclei dispersed on the surface. Above a given percolation threshold, a growing percolation cluster progressively discharges an increasing portion of this electret surface, thus reducing the surface potential of the charged electret, the remaining surface potential being unaltered. The interest of this kind of model, even quite simplified, is to introduce in the analysis the local heterogeneity of the surface conductivity, which certainly often plays a great part in the surface decay process.

### *7.3 Charge surface migration*

On an insulator assumed to be devoid of any surface conductivity, surface charges may have a lateral mobility allowing them to migrate under the influence of their own field, due to the repulsion force between them. This may occur near a triple junction through injection from an electrode, or from a surface charge distribution deposited on a surface by a transfer through the gas, or by rubbing. However, even assuming an elementary description of the charge motion as it has been done for electrostatic models (considering a constant mobility), the calculation of the charge distribution evolution and potential decay is quite complicated. We will just present here a few elements, while the interested reader may consult the few detailed papers partly or entirely devoted to this problem. A model of charge migration under its own field on a surface of a grounded insulator has been developed six decades ago by Geurst to analyze charge migration in a field-effect transistor channel [118], then other models of surface space charge limited injection have been produced by Wintle and coworkers [44,55,111,119].

An analysis of the specific question of the charge decay by this process may be found in [44,55,111]. In [44], for instance, simulations of the surface charge distribution evolution for three different geometries are reported. Considering a surface gap between electrodes, at the separation surface of two half-plane dielectrics, charge injected at the left electrode tends to evolve, after short-circuiting the electrodes, towards a symmetrical distribution in the gap, as shown Figure 13.

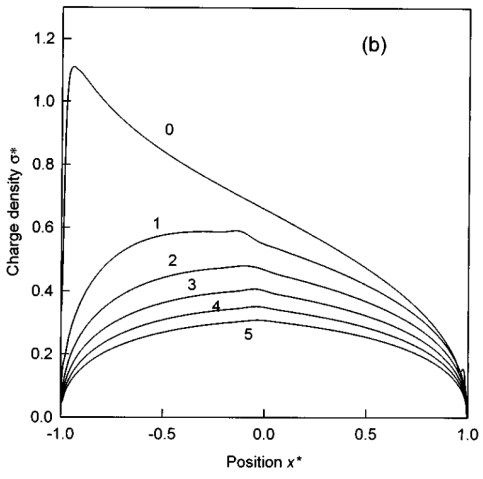

Figure 13 : Simulation of the charge distribution evolution between surface electrodes [44]

This figure strongly suggests an evolution comparable to what happens on a slightly conductive surface. The first part of the decay is dominated by a fast reorganization of the surface charge distribution accompanying the mean decrease of the charge density, which leads to a symmetrical charge distribution, and to a self-similar regime.

Assuming the insulator being grounded on its back electrode, the equation (33) is still valid, but the continuity equation leads to a different result for a space charge driven conductivity:

$$\frac{\partial V}{\partial t} = \frac{d}{\varepsilon}\frac{\partial \sigma}{\partial t} = -\frac{d\mu}{\varepsilon}\frac{\partial(\sigma E_x)}{\partial x} = -\mu\frac{\partial(VE_x)}{\partial x} = \frac{\mu}{2}\frac{\partial^2 V^2}{\partial x^2} \tag{42}$$

Looking as above for self-similar solutions for the long times ($V = V_0 f(t) g(x)$), we obtain from (42) :

$$g(x)\frac{\partial f(t)}{\partial t} = V_0\frac{\mu}{2} f(t)^2\frac{\partial^2 g(x)^2}{\partial x^2} \tag{43}$$

From this equation we may deduce that the decay should be hyperbolic when the shape of the distribution is stationary:

$$f(t) = at^{-1} \tag{44}$$

Assuming a self-similar regime, the physical reason why the charge decay should follow a hyperbolic time dependence is exactly the same than when bulk injection is considered. In both cases, the charge distribution shape being fixed, the amount of charge leaving the insulator is proportional to the product of the charge velocity by the charge density in the vicinity of the electrodes. Assuming a constant mobility and a constant shape of the distribution, both quantities are proportional to the total charge in the sample (or on its surface), and their product – and hence the charge time derivative - to the square of this charge. The hyperbolic nature of the asymptotic decay is also found in [111] for the charge migration case but the author conclude by an interrogation about the hypothesis of the existence of a self-similar regime : *"it is an open question whether there is a self-similar solution for the charge driven case with solid electrodes. The same is true for the common practical arrangement of an insulating sheet lying on a ground plane"*. The nonlinear nature of the differential equation (43) makes indeed impossible to find an analytical solution for the distribution in the self-similar regime, if it does exist. However data from simulation (as in Figure 13) and experiments show that the convergence towards such a regime is usually found quite rapidly.

### *7.4 Data on real materials*

The surface conductivity may be measured according to ASTM standards [66] using a setup of concentric electrodes on the same side of the insulator. It is obviously strongly depending on the preparation of the samples, the existence of a pollution layer on their surfaces, their ageing, etc. Dry and clean insulating polymers are usually hydrophobic and their typical surface resistivity values are in the range $10^{-19}$- $5.10^{-17}$ $\Omega^{-1}$ in relatively dry atmospheres (RH < 50%). In the literature may be found for instance $10^{-19}$ $\Omega^{-1}$ for LDPE at 80% RH [120], $10^{-18}$ $\Omega^{-1}$ for epoxy in dry SF6 [109,121], $5.10^{-17}$ $\Omega^{-1}$ for epoxy in air at 50% RH [122], $5.10^{-17}$ $\Omega^{-1}$ for Teflon in air at 40% RH [123], from $5.10^{-19}$ to $3.2\ 10^{-17}$ on silicone rubber [124].

Humidity has obviously a decisive influence on surface conductivity. An exponential dependence of the conductivity on the relative humidity is found on various materials. An ancient publication [125] reports this property on classical insulating materials as wool, cotton or cellulose, but also that a high moisture sensitivity or even water solubility does not necessarily confer good antistatic properties to a given polymer. It also shows that positive and negative charging usually do not lead to the same result [126]. This result cannot be obtained by assuming an intrinsic surface charge conductivity, even humidity dependent, of the materials. An exponential dependence of the surface conductivity with the relative humidity is also found on PMMA [116], Teflon or quartz [123]. However for quartz, a deviation to this effect is reported at low relative humidity, which is interpreted by a calculation showing that the threshold of the exponential dependence on quartz is obtained when the first monolayer of water molecules on the surface is complete. According to the authors, this threshold is not observed on Teflon due to its strongly hydrophobic character.

Concerning charge migration on dry insulators, either injected from electrodes or by self-repulsion of a surface charge deposited on a surface, the results, as shown by [44], are quite contradictory and depend on the experimental configuration, surface state, etc. Some results seem to imply that charge lateral migration is quite difficult on dry polymers and depends on temperature. For instance, according to [43], on PET, this migration is responsible for most of the charge decay at 120°C (with a time constant of about 500s), however no lateral migration may be detected at ambient temperature, even after 24 hours.

Concerning the shape of the charge distribution, the theoretical prediction of a tendency towards a self-similar cosine shape, when the decay process is due to surface conductivity, is confirmed by potential scans on the surface, as shown on Figure 14 for a silica surface in ambient air [113]. The same result is observed in [127].

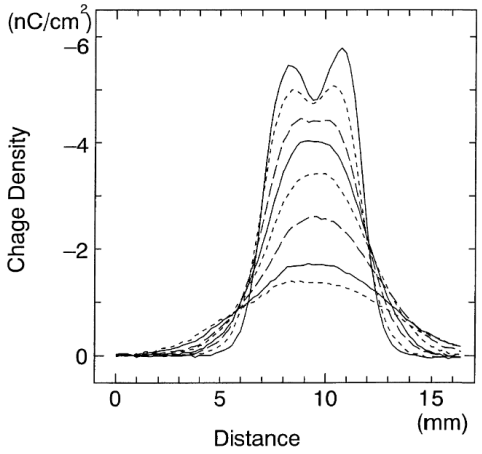


Figure 14 : Evolution of the lateral charge density profile due to surface conductivity on silica [113]

## 8 Conclusions

Some general conclusions may be drawn from this quite long journey among the various processes that could pilot charge decay on dielectrics. Those which may lead to a time power law dependence of the decay rate (including hyperbolic decay) are listed with their main characteristics in Table 1, while the physical causes of exponential and linear decays are listed Table 2.

| Physical cause for the decay | Key parameter | Slope of $\log(dV/dt) = f(logt)$ | | Significance of characteristic time $\tau$ | $dV/dt$ dependence on initial potential and thickness | | | |
|---|---|---|---|---|---|---|---|---|
| | | $t \ll \tau$ | $t \gg \tau$ | | $V_0$ | | $L$ at fixed $V_0/L$ | |
| *Charge injection (Figure 8 – left)* | Charge mobility | 0 | $-2$ | Transit time $\tau \propto L^2/V_0$ | $t \ll \tau$ | $t \gg \tau$ | $t \ll \tau$ | $t \gg \tau$ |
| *Charge injection (dispersive) (Figure 8 – right)* | Charge mobility + trap distribution | For an exponential trap energy distribution ($\alpha = kT/W_0$) | | Transit time $\tau \propto \left(L^2/V_0\right)^{1/\alpha}$ | $\propto {V_0}^2$ | 0 | $\propto L^{-1}$ | $\propto L^2$ |
| *Volume detrapping (depletion discharge – see section 5)* | Trap distribution | $-1 + kT/W_0$ | $-1 - kT/W_0$ | Depletion time $\tau \propto \left(V_0/L^2\right)^{1/\alpha}$ | $t \ll \tau$ 0 | $t \gg \tau$ $\propto {V_0}^2$ | $t \ll \tau$ $\propto L^2$ | $t \gg \tau$ $\propto L^{-1}$ |
| *Charge detrapping (no retrapping – see Figure 10)* | Trap distribution | $d\log N\left(kT\ln(\nu t)\right)/d\log t$ | | Detrapping time for maximum trap density | $\propto V_0$ | | $\propto L$ | |
| *Dipolar polarization (section 6)* | Relaxation function | For a Cole-Cole relaxation with $\alpha \in ]0,1[$ $-1+\alpha$ | $-1-\alpha$ | Characteristic relaxation time | $\propto V_0$ | | $\propto L$ | |
| *Ohmic surface far from electrodes (section 7.2)* | Surface conductivity | Depends on initial surface distribution | $-2$ | Self-similar distribution reached | $\propto V_0$ | | - | |
| *Surface charge migration (section 7.3)* | Charge surface mobility | | $-2$ | Self-similar distribution reached | $\propto {V_0}^2$ | | $\propto L^2$ | |

Table 1: Possible causes for a power law behavior of the potential decay rate

| Physical cause for the decay | Key parameter | Shape of the decay | $dV/dt$ dependence on | |
|---|---|---|---|---|
| | | | $V_0$ | $L$ at fixed $V_0/L$ |
| *Ionic current in air (section 3)* | Ion generation | ≈ linear (decrease of collection volume) | Slight (increase of collection volume) | |
| *Ohmic conduction (volume)* | | Exponential | | |

| | | | | |
|---|---|---|---|---|
| *(section 5)* | Volume conductivity | | $\propto V_0$ | $\propto L$ |
| *Ohmic surface conductivity above a grounded plane or between electrodes (section 7.2)* | Surface conductivity | Exponential | $\propto V_0$ | $\propto L^3$ |

Table 2 : Causes of linear and exponential decay

A striking feature of these results is that quite different processes may lead to a similar potential decay shape. Hence it is quite easy to misinterpret the experimental data. In our opinion, the first step in interpreting the data, on a given material, is to determine what kind of process is responsible for the decay. Checking the influence of gaseous neutralization or surface conductivity may usually be performed quite easily by checking the effect of changes in the measurement setup, or in the experimental conditions (using a field mill instead of an electrostatic probe to increase a possible gaseous neutralization process, adjoining a surface ground electrode to promote surface conduction, etc.). The existence of surface conduction or migration may also be detected by potential scans after depositing a sharp patch of charge at the beginning of the experiment.

The power law behavior, due to trapping, is observed as well for internal relaxation processes, and for external charge injection into the material. The characteristic time that may be observed could be a transit time, as well as a characteristic relaxation time, or a characteristic detrapping time. Hence the shape of the decay and a curve fitting procedure could not avoid confusion, and specific experiments should be here also performed to decide. Charge injection processes should be detected by field non-linearity and above all by a dependence on the electrode material. Polarization may also be evidenced by leaving an air gap when an external field is applied to the sample. A general and simple classification, at ambient temperature, coming from the author's personal experience, and from what has been described here, is the following:

- On a charged surface far from the ground, either on a thick (>1cm) grounded insulator, or on a charged web, gaseous and surface neutralization processes are dominant.
- On a charged insulator of "intermediate thickness" (from 0,5 mm to 1cm) and on films (<500µm) at moderate fields (below 10 kV/mm), volume polarization processes dominate
- On a charged thin film at high fields (above 10kV/mm), charge injection has to be taken to account, especially during charging and immediately after.

This classification neglects however what may be the most important: the material. The above classification may not be pertinent for some materials or situations. For instance, concerning electrets, where a maximal long-time charge stability is sought, the stability, even at quite moderate fields, is strongly different in positive and negative polarity, for instance in PTFE [128], FEP [7] or SiO2 [129]. It is clear for these excellent insulators where, after annealing allowing deep retrapping of the mobile carriers, intrinsic volume polarization processes as well as intrinsic charge motion are almost inexistent, even at quite high temperatures, so that other processes, as surface charge injection, may dominate on the very long time. This review has been written to identify and analyze the different mechanisms possibly involved in the charge decay, not to provide answers to the question of what happens concerning a given material in a given situation. For this purpose, the reader has to refer to the literature and to well-designed experiments.

An aspect that has not been treated in this review mainly dedicated to the physical mechanisms responsible for the time dependence of the isothermal charge decay is the influence of temperature. We will just underline here that all the processes described here are influenced by temperature. In general, heating promotes charge injection, dipolar motion and detrapping.

Another topic which is related to the time dependence of the decay is the memory effect. Due to the particular shape of the decay usually involving power laws, successive charging pulses on an insulator will lead to a progressive decrease of the potential decay rate and a progressive charge buildup, as may be seen on Figure 15. This may be computed using the superposition principle, assuming a linear behavior of the insulator. The existence in parallel of a volume conduction will limit this phenomenon (dotted lines). This memory effect is also responsible for the return voltage, topic we treated in details in another article [130].

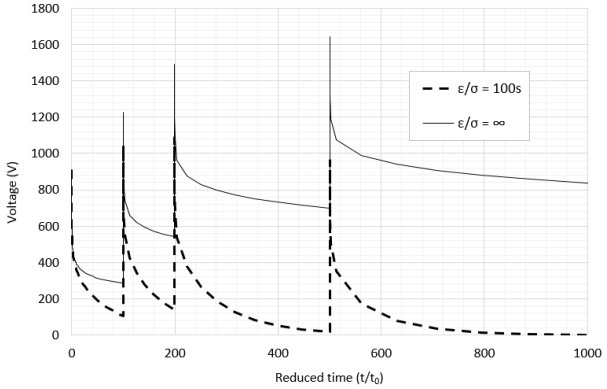

Figure 15 : Voltage build up on a dispersive (α = 0.2) insulator subjected to several current pulses with or without conductivity (σ) [90]

To conclude this review, we may remark that, despite an effort to check the 21th century literature as carefully as possible, it relies mainly to quite ancient research works. Since a large part of them is unknown to many researchers using charge decay models, we believe that this review may be of any use. We may also conclude that few theoretical advances were accomplished these last years concerning this topic. This might be because many of the theoretical problems discussed here have already been solved, but many others certainly also remain open to research.

*"How fast does a charge decay?"* was the title of a technical magazine chronicle in 2012 [131]. Its conclusion was: *"Although we can accurately predict the current* I *through a resistor with the resistance* R *from a voltage supply with output voltage* V*, we have to accept that static electricity is a little more complicated (and interesting). We also have to accept the fact that there's no way you can predict the decay behavior of a manufactured item placed in an arbitrary environment by doing some laboratory measurements on a sample of the material of said item."*

This difficulty to predict is still here, due to the complex combination of physical phenomena involved in static electricity. However improving our understanding and models of each of these phenomena remains necessary (and interesting).

**References**


[1] G. Lüttgens, N. Wilson, Electrostatic hazards, Butterworth Heinemann, Oxford; Boston, 1997.

[2] J.R. Dennison, Dynamic Interplay Between Spacecraft Charging, Space Environment Interactions, and Evolving Materials, IEEE Trans. Plasma Sci. 43 (2015) 2933–2940. https://doi.org/10.1109/TPS.2015.2434947.

[3] E.A. Amerasekera, C. Duvvury, ESD in silicon integrated circuits, 2nd ed, J. Wiley, Chichester, 2010.

[4] F. Wang, T. Zhang, J. Li, K.M. Zeeshan, L. He, Z. Huang, Y. He, DC breakdown and flashover characteristics of direct fluorinated epoxy/$Al_2O_3$ nanocomposites, IEEE Trans. Dielect. Electr. Insul. 26 (2019) 702–737. https://doi.org/10.1109/TDEI.2018.007642.

[5] F. Wang, F. Liang, S. Chen, L. Zhong, Q. Sun, B. Zhang, P. Xiao, Effect of Surface Charges on Flashover Voltage - An Examination Considering Charge Decay Rates, IEEE Trans. Dielect. Electr. Insul. 28 (2021) 1053–1060. https://doi.org/10.1109/TDEI.2021.009511.

[6] Y. Liu, G. Wu, G. Gao, J. Xue, Y. Kang, C. Shi, Surface charge accumulation behavior and its influence on surface flashover performance of Al $_2$ O $_3$ -filled epoxy resin insulators under DC voltages, Plasma Sci. Technol. 21 (2019) 055501. https://doi.org/10.1088/2058-6272/aafdf7.

[7] A. Gerlach, M. Liebler, G.M. Sessler, H. Von Seggern, B. Scheufele, E. Hirth, Comparative analysis of isothermal decay of the surface potential of fluoroethylenepropylene electrets and of the sensitivity of electret microphones at elevated temperature, AIP Advances 10 (2020) 095313. https://doi.org/10.1063/5.0016219.

[8] X. Li, Y. Wang, M. Xu, Y. Shi, H. Wang, X. Yang, H. Ying, Q. Zhang, Polymer electrets and their applications, J of Applied Polymer Sci 138 (2021) 50406. https://doi.org/10.1002/app.50406.

[9] C. Wang, H. Guo, P. Wang, J. Li, Y. Sun, D. Zhang, An Advanced Strategy to Enhance TENG Output: Reducing Triboelectric Charge Decay, Advanced Materials 35 (2023) 2209895. https://doi.org/10.1002/adma.202209895.

[10] O. Tilmatine, T. Zeghloul, K. Medles, L. Dascalescu, A. Fatu, Effect of ambient air relative humidity on the triboelectric properties of Polypropylene and Polyvinyl Chloride slabs, Journal of Electrostatics 115 (2022) 103651. https://doi.org/10.1016/j.elstat.2021.103651.

[11] R. Kohlrausch, Theorie des elektrischen Rückstandes in der Leidener Flasche, Ann. Phys. Chem. 167 (1854) 179–214. https://doi.org/10.1002/andp.18541670203.

[12] G. Williams, D.C. Watts, Non-symmetrical dielectric relaxation behaviour arising from a simple empirical decay function, Trans. Faraday Soc. 66 (1970) 80. https://doi.org/10.1039/tf9706600080.

[13] J. Curie, Recherches sur le pouvoir inducteur spécifique et sur la conductibilité des corps cristallisés, Thèse de doctorat, Faculté des sciences de Paris, 1888.

[14] E.R. V. Schweidler, Studien über die Anomalien im Verhalten der Dielektrika, Ann. Phys. 329 (1907) 711–770. https://doi.org/10.1002/andp.19073291407.

[15] B. Gross, Über die Anomalien der festen Dielektrika, Zeitschrift für Physik 107 (1937) 217–234. https://doi.org/10.1007/BF01330365.

[16] B. Gross, On discharge voltage and return voltage curves for absorptive capacitors, Physical Review 62 (1942) 383.

[17] F.M. De Oliveira Castro, Zur Theorie der dielektrischen Nachwirkung, Z. Physik 114 (1939) 116–126. https://doi.org/10.1007/BF01340237.

[18] D.W. Vance, Surface Charging of Insulators by Ion Irradiation, Journal of Applied Physics 42 (1971) 5430. https://doi.org/10.1063/1.1659961.

[19] I. Chen, R.L. Emerald, J. Mort, Dependence of xerographic discharge characteristics on carrier mobilities, Journal of Applied Physics 44 (1973) 3490–3495.

[20] H. Scher, E. Montroll, Anomalous transit-time dispersion in amorphous solids, Physical Review B 12 (1975) 2455–2477. https://doi.org/10.1103/PhysRevB.12.2455.

[21] P.K. Watson, The energy distribution of localized states in polystyrene, based on isothermal discharge measurements, Journal of Physics D: Applied Physics 23 (1990) 1479–1484. https://doi.org/10.1088/0022-3727/23/12/002.

[22] P.K. Watson, The transport and trapping of electrons in polymers, IEEE Trans. Dielect. Electr. Insul. 2 (1995) 915–924. https://doi.org/10.1109/94.469986.

[23] I.P. Batra, K.K. Kanazawa, H. Seki, Discharge Characteristics of Photoconducting Insulators, Journal of Applied Physics 41 (1970) 3416–3422. https://doi.org/10.1063/1.1659433.

[24] K.K. Kanazawa, I.P. Batra, H.J. Wintle, Decay of Surface Potential in Insulators, Journal of Applied Physics 43 (1972) 719. https://doi.org/10.1063/1.1661182.

[25] S.J. Fox, Decay of surface potential in electrophotography: Single-carrier case, Journal of Applied Physics 45 (1974) 610. https://doi.org/10.1063/1.1663292.

[26] A. Reiser, M.W.B. Lock, J. Knight, Migration and trapping of extrinsic charge carriers in polymer films, Trans. Faraday Soc. 65 (1969) 2168. https://doi.org/10.1039/tf9696502168.

[27] R.H. Young, Kinetics of xerographic discharge by surface charge injection, Journal of Applied Physics 72 (1992) 2993–3004. https://doi.org/10.1063/1.351507.

[28] M.M. Perlman, S. Bamji, Applicability of the Scher-Montroll model to transient photocurrent and surface potential decay in insulators, Applied Physics Letters 33 (1978) 581–583. https://doi.org/10.1063/1.90467.

[29] A. Kubilius, B. Petretis, V.I. Archipov, A.I. Rudenko, Dark discharge of surface potential in disordered materials (a-Se), J. Phys. D: Appl. Phys. 18 (1985) 901–909. https://doi.org/10.1088/0022-3727/18/5/014.

[30] Arkhipov, V. I., Rudenko, A. I., Influence of the space charge on dispersive transport, Sov. Phys. Semicond. 16 (1982) 1153–1156.

[31] M. Ieda, G. Sawa, U. Shinohara, A Decay Process of Surface Electric Charges across Poyethylene Film, Jpn. J. Appl. Phys. 6 (1967) 793. https://doi.org/10.1143/JJAP.6.793.

[32] M. Ieda, G. Sawa, U. Shinohara, Decay of electric charges on polymeric films, Electrical Engineering in Japan 88 (1968).

[33] H.J. Wintle, Decay of Static Electrification by Conduction Processes in Polyethylene, Journal of Applied Physics 41 (1970) 4004. https://doi.org/10.1063/1.1658402.

[34] H.J. Wintle, Surface-Charge Decay in Insulators with Nonconstant Mobility and with Deep Trapping, Journal of Applied Physics 43 (1972) 2927. https://doi.org/10.1063/1.1661633.

[35] T.J. Sonnonstine, M.M. Perlman, Surface-potential decay in insulators with field-dependent mobility and injection efficiency, Journal of Applied Physics 46 (1975) 3975. https://doi.org/10.1063/1.322148.

[36] R.M. Hill, Relaxation of surface charge, Journal of Physics C: Solid State Physics 8 (1975) 2488.

[37] R. Coelho, L. Levy, D. Sarrail, Charge decay measurements and injection in insulators, Journal of Physics D: Applied Physics 22 (1989) 1406–1409. https://doi.org/10.1088/0022-3727/22/9/029.

[38] H. Von Berlepsch, Interpretation of surface potential kinetics in HDPE by a trapping model, Journal of Physics D: Applied Physics 18 (1985) 1155.

[39] E.A. Baum, T.J. Lewis, R. Toomer, Decay of electrical charge on polyethylene films, Journal of Physics D: Applied Physics 10 (1977) 487.

[40] K.J. Kao, S.S. Bamji, M.M. Perlman, Thermally stimulated discharge current study of surface charge release in polyethylene by corona-generated excited molecules, and the crossover phenomenon, Journal of Applied Physics 50 (1979) 8181. https://doi.org/10.1063/1.325958.

[41] S. Haridoss, Vibrationally excited diatomic molecules as charge injectors during corona charging of polymer films, Journal of Applied Physics 53 (1982) 6106. https://doi.org/10.1063/1.331564.

[42] A. Kumar, M.M. Perlman, Sliding-friction electrification of polymers and charge decay, J Polym Sci B Polym Phys 30 (1992) 859–863. https://doi.org/10.1002/polb.1992.090300807.

[43] E.A. Baum, T.J. Lewis, R. Toomer, The lateral motion of charge on thin films of polyethylene terephthalate, Journal of Physics D: Applied Physics 11 (1978) 963.

[44] M.P. Pépin, H.J. Wintle, Charge injection and conduction on the surface of insulators, Journal of Applied Physics 83 (1998) 5870–5879. https://doi.org/10.1063/1.367448.

[45] H.J. Wintle, Charge motion and trapping in insulators: surface and bulk effects, Dielectrics and Electrical Insulation, IEEE Transactions On 6 (1999) 1–10.

[46] G.M. Sessler, Charge storage in dielectrics, IEEE Transactions on Electrical Insulation 24 (1989) 395–402. https://doi.org/10.1109/14.30879.

[47] G.A. Mekishev, Surface Processes in Charge Decay of Electrets, in: B.M. Caruta (Ed.), Trends in Materials Science Research, Nova Science Publishers, New York, 2006.

[48] J. Matallana, J. Bigarre, P. Hourquebie, R. Coelho, H. Janah, P. Mirebeau, S. Agnel, A. Toureille, Recent experiments on space charge and transport in polyethylene under high DC field, in: 2001 Ann. Rept. CEIDP, IEEE, 2001: pp. 488–491. https://doi.org/10.1109/CEIDP.2001.963587.

[49] J. Kindersberger, C. Lederle, Surface charge decay on insulators in air and sulfurhexafluorid-Part I: Simulation, Dielectrics and Electrical Insulation, IEEE Transactions On 15 (2008) 941–948.

[50] J. Kindersberger, C. Lederle, Surface charge decay on insulators in air and sulfurhexafluorid-part II: measurements, Dielectrics and Electrical Insulation, IEEE Transactions On 15 (2008) 949–957.

[51] K. Robinson, Charge Relaxation Due to Surface Conduction on an Insulating Sheet Near a Grounded Conducting Plane, IEEE Trans. on Ind. Applicat. 40 (2004) 1231–1238. https://doi.org/10.1109/TIA.2004.834134.

[52] K.S. Robinson, Variation in Static Decay Time With Surface Resistivity, IEEE Trans. on Ind. Applicat. 49 (2013) 2300–2307. https://doi.org/10.1109/TIA.2013.2260312.

[53] V.I. Mikla, V.V. Mikla, Xerographic spectroscopy of gap states in Se-rich amorphous semiconductors review, Journal of Non-Crystalline Solids 357 (2011) 3675–3688. https://doi.org/10.1016/j.jnoncrysol.2011.07.018.

[54] N. Knorr, S. Rosselli, G. Nelles, Surface-potential decay of biased-probe contact-charged amorphous polymer films, Journal of Applied Physics 107 (2010) 054106. https://doi.org/10.1063/1.3309763.

[55] H.J. Wintle, Interpretation of atomic force microscope (AFM) signals from surface charge on insulators, Meas. Sci. Technol. 8 (1997) 508–513. https://doi.org/10.1088/0957-0233/8/5/007.

[56] P. Molinié, Charge injection in corona-charged polymeric films: potential decay and current measurements, Journal of Electrostatics 45 (1999) 265–273.

[57] P. Llovera, P. Molinié, New methodology for surface potential decay measurements: application to study charge injection dynamics on polypropylene films, Dielectrics and Electrical Insulation, IEEE Transactions On 11 (2004) 1049–1056.

[58] P. Zhang, F. Zhou, C. Zhang, Z. Yan, J. Li, H. Jin, H. Zhang, J. Lu, Charge trapping characteristics of alumina based ceramics, Ceramics International 44 (2018) 12112–12117. https://doi.org/10.1016/j.ceramint.2018.03.232.

[59] A. Rychkov, A. Kuznetsov, A. Gulyakova, D. Rychkov, Surface Potential Decay of Corona Charged Polyethylene Films: Influence of Deep Surface Traps, IEEE Trans. Dielect. Electr. Insul. 28 (2021) 1933–1937. https://doi.org/10.1109/TDEI.2021.009698.

[60] P. Molinié, Measuring and modeling transient insulator response to charging: the contribution of surface potential studies, Dielectrics and Electrical Insulation, IEEE Transactions On 12 (2005) 939–950.

[61] P. Molinié, Modeling static charge dissipation on solids: An historical perspective, Journal of Electrostatics 71 (2013) 591–596. https://doi.org/10.1016/j.elstat.2012.12.001.

[62] IEC/TR 61340-1, Technical Report. Electrostatics. Part1 : Electrostatic phenomena. Principles and measurements, (2012).

[63] C.T. Lynch, CRC handbook of materials science: material composites and refractory materials, 1st ed., CRC Press, Boca Raton, 2020.

[64] S. Fakhfakh, O. Jbara, S. Rondot, A. Hadjadj, J.M. Patat, Z. Fakhfakh, Analysis of electrical charging and discharging kinetics of different glasses under electron irradiation in a scanning electron microscope, Journal of Applied Physics 108 (2010) 093705. https://doi.org/10.1063/1.3499692.

[65] R.C. Weatherwax, A.J. Stamm, The electrical resistivity of resin-treated wood and laminated hydrolyzed-wood and paper-base plastics, Electr. Eng. 64 (1945) 833–838. https://doi.org/10.1109/EE.1945.6441387.

[66] ASTM, D257 - Standard test methods for DC resistance or conductance of Insulating Materials, (1991).

[67] A.K. Jonscher, The 'universal' dielectric response, Nature 267 (1977) 673–679. https://doi.org/10.1038/267673a0.

[68] S. Kumara, X. Xu, T. Hammarström, Y. Ouyang, A.M. Pourrahimi, C. Müller, Y.V. Serdyuk, Electrical Characterization of a New Crosslinked Copolymer Blend for DC Cable Insulation, Energies 13 (2020) 1434. https://doi.org/10.3390/en13061434.

[69] H. Sjostedt, S.M. Gubanski, Y.V. Serdyuk, Charging characteristics of EPDM and silicone rubbers deduced from surface potential measurements, Dielectrics and Electrical Insulation, IEEE Transactions On 16 (2009) 696–703.

[70] P. Molinié, M. Goldman, J. Gatellet, Surface potential decay on corona-charged epoxy samples due to polarization processes, Journal of Physics D: Applied Physics 28 (1995) 1601–1610. https://doi.org/10.1088/0022-3727/28/8/009.

[71] P. Llovera, P. Molinié, A. Soria, A. Quijano, Measurements of electrostatic potentials and electric fields in some industrial applications: Basic principles, Journal of Electrostatics 67 (2009) 457–461. https://doi.org/10.1016/j.elstat.2009.01.004.

[72] A. Mikiver, Measurements of Air Ion Concentrations and Electric Field Strengths for HVDC Applications Master's thesis in Electric Power Engineering, Masters Thesis, Chalmers University of Technology, 2017.

[73] C. Heinert, R.M. Sankaran, D.J. Lacks, Decay of electrostatic charge on surfaces due solely to gas phase interactions, Journal of Electrostatics 115 (2022) 103663. https://doi.org/10.1016/j.elstat.2021.103663.

[74] R. Rosen, E.P. George, Ion distributions in plane and cylindrical chambers, Phys. Med. Biol. 20 (1975) 990–1002. https://doi.org/10.1088/0031-9155/20/6/011.

[75] B. Zhang, G. Zhang, Interpretation of the surface charge decay kinetics on insulators with different neutralization mechanisms, Journal of Applied Physics 121 (2017) 105105. https://doi.org/10.1063/1.4978001.

[76] P. Llovera-Segovia, P. Molinié, V. Fuster, A. Quijano-López, Electrostatic potential measurement of floating conductive objects: some theoretical considerations and experimental results., Journal of Electrostatics (This issue) (2024).

[77] T.J.M. Gaertner, Th. Stoop, J. Tom, H.F.A. Verhaart, A.J.L. Verhage, Decay of surface charges on insulators in SF6, in: 1984 IEEE International Conference on Electrical Insulation, IEEE, Montreal Quebec, Canada, 1984: pp. 208–213. https://doi.org/10.1109/EIC.1984.7465181.

[78] R. Coelho, B. Aladenize, Contribution to the analysis of the decay of charged samples, in: IEEE, 1995: pp. 621–625. https://doi.org/10.1109/CEIDP.1995.483802.

[79] M. Campos, J.A. Giacometti, Surface-potential decay in naphthalene, Applied Physics Letters 32 (1978) 794. https://doi.org/10.1063/1.89933.

[80] G. Chen, A new model for surface potential decay of corona-charged polymers, Journal of Physics D: Applied Physics 43 (2010) 055405. https://doi.org/10.1088/0022-3727/43/5/055405.

[81] Z. Xu, L. Zhang, G. Chen, Decay of electric charge on corona charged polyethylene, Journal of Physics D: Applied Physics 40 (2007) 7085–7089. https://doi.org/10.1088/0022-3727/40/22/033.

[82] K.K. Kanazawa, I.P. Batra, Deep-Trapping Kinematics, Journal of Applied Physics 43 (1972) 1845–1853. https://doi.org/10.1063/1.1661408.

[83] M. Campos, Surface-potential decay in insulators with deep traps, Journal of Applied Physics 52 (1981) 4546. https://doi.org/10.1063/1.329328.

[84] R.T. Sibatov, V.V. Uchaikin, Fractional differential approach to dispersive transport in semiconductors, Physics-Uspekhi 52 (2009) 1019–1043. https://doi.org/10.3367/UFNe.0179.200910c.1079.

[85] V.I. Arkhipov, J.A. Popova, A.I. Rudenko, Space-charge perturbed dispersive transport in disordered dielectrics, Journal of Electrostatics 18 (1986) 23–37.

[86] J. Kyokane, K. Yoshino, Y. Inuishi, R. Coelho, A consideration on decay process of an accumulated charge of polymer surfaces, Electron. Commun. Jpn. 102 (1982) 25–32. https://doi.org/10.1002/ecja.4391020105.

[87] M. Campos, J.A. Giacometti, M. Silver, Deep exponential distribution of traps in naphthalene, Applied Physics Letters 34 (1979) 226. https://doi.org/10.1063/1.90739.

[88] R. Toomer, T.J. Lewis, Charge trapping in corona-charged polyethylene films, Journal of Physics D: Applied Physics 13 (1980) 1343.

[89] G. Teyssedre, F. Zheng, L. Boudou, C. Laurent, Charge trap spectroscopy in polymer dielectrics: a critical review, Appl. Phys. (2021) 31.

[90] P. Molinié, A Panorama of Electrical Conduction Models in Dielectrics, With Application to Spacecraft Charging, IEEE Transactions on Plasma Science 43 (2015) 2869–2874. https://doi.org/10.1109/TPS.2015.2461625.

[91] J.G. Simmons, M.C. Tam, Theory of isothermal currents and the direct determination of trap parameters in semiconductors and insulators containing arbitrary trap distributions, Physical Review B 7 (1973) 3706.

[92] V. Halpern, Transient photoconductivity and demarcation energies in amorphous semiconductors, Philosophical Magazine B 51 (1985) L49–L52. https://doi.org/10.1080/13642818508244479.

[93] V. Adamec, J.H. Calderwood, The interpretation of potential decay on the surface of a charged dielectric specimens, Journal of Physics D: Applied Physics 20 (1987) 803.

[94] S.O. Kasap, M. Baxendale, C. Juhasz, Evidence for field-assisted thermal emission of holes from deep mobility gap states in amorphous semiconductors from xerographic dark discharge measurements, Journal of Applied Physics 62 (1987) 171. https://doi.org/10.1063/1.339176.

[95] D.M. Taylor, T.P.T. Williams, Decay of surface charge in the presence of a time-dependent bulk conductivity, Journal of Physics C: Solid State Physics 11 (1978) 111.

[96] D.K. Das-Gupta, Decay of electrical charges on organic synthetic polymer surfaces, Electrical Insulation, IEEE Transactions On 25 (1990) 503–508.

[97] K.S. Cole, R.H. Cole, Dispersion and Absorption in Dielectrics I. Alternating Current Characteristics, The Journal of Chemical Physics 9 (1941) 341–351. https://doi.org/10.1063/1.1750906.

[98] S. Havriliak, S. Negami, A complex plane representation of dielectric and mechanical relaxation processes in some polymers, Polymer 8 (1967) 161–210. https://doi.org/10.1016/0032-3861(67)90021-3.

[99] F. Mainardi, A. Consiglio, The Pioneers of the Mittag-Leffler Functions in Dielectrical and Mechanical Relaxation Processes, WSEAS Trans. Mathematics 19 (2020) 289–300. https://doi.org/10.37394/23206.2020.19.29.

[100] P. Molinié, Dielectric relaxation in open circuit: Theory, simulations, and some experiments, Journal of Applied Physics 134 (2023) 134101. https://doi.org/10.1063/5.0170968.

[101] R. Garrappa, F. Mainardi, G. Maione, Models of Dielectric Relaxation Based on Completely Monotone Functions, FCAA 19 (2016) 1105–1160. https://doi.org/10.1515/fca-2016-0060.

[102] A.K. Jonscher, Dielectric relaxation in solids, Journal of Physics D: Applied Physics 32 (1999) R57.

[103] G.G. Raju, Dielectrics in electric fields, Second edition, CRC Press, Taylor & Francis Group, Boca Raton London New York, 2017.

[104] U. Lachish, I.T. Steinberger, Electrical current measurements on polystyrene films, Journal of Physics D: Applied Physics 7 (1974) 58.

[105] P.J. Atkinson, R.J. Fleming, Origin of absorption and resorption currents in the co-polymer poly (hexafluoropropylene-tetrafluoroethylene), Journal of Physics D: Applied Physics 9 (1976) 2027.

[106] P.J. Atkinson, R.J. Fleming, Surface component of vacuum absorption and resorption currents in polymers. I. Origin and magnitude, J. Phys. D: Appl. Phys. 13 (1980) 625–638. https://doi.org/10.1088/0022-3727/13/4/016.

[107] H.J. Wintle, T.C. Chapman, Comment on ''Anisotropy study of electrical conduction in oriented polymers. I. Analysis of bulk electrical conduction parallel to the surface of film'', Journal of Applied Physics 51 (1980) 3435–3436. https://doi.org/10.1063/1.328027.

[108] T.C. Chapman, H.J. Wintle, Dielectric absorption currents and surface charge on polymeric insulators, Journal of Applied Physics 51 (1980) 4898–4904. https://doi.org/10.1063/1.328328.

[109] H. Iwabuchi, T. Donen, S. Matsuoka, A. Kumada, K. Hidaka, Y. Hoshina, M. Takei, Influence of surface-conductivity nonuniformity on charge accumulation of GIS downsized model spacer under DC field application, Electrical Engineering Japan 181 (2012) 29–36. https://doi.org/10.1002/eej.22272.

[110] S. Okabe, Phenomena and mechanism of electric charges on spacers in gas insulated switchgears, IEEE Trans. Dielect. Electr. Insul. 14 (2007) 46–52. https://doi.org/10.1109/TDEI.2007.302871.

[111] H.J. Wintle, M.P. Pépin, Decay of surface charge between electrodes on insulator surfaces, Journal of Electrostatics 48 (2000) 115–126. https://doi.org/10.1016/S0304-3886(99)00058-3.

[112] A. Crisci, B. Gosse, J.-P. Gosse, V. Ollier-Duréault, Surface-potential decay due to surface conduction, Eur. Phys. J. AP 4 (1998) 107–116. https://doi.org/10.1051/epjap:1998249.

[113] Y. Hori, The lateral migration of surface charges on poly(methyl methacrylate) graft-copolymerized onto polypropylene film, and its dependency on relative humidity, Journal of Electrostatics 48 (2000) 127–143.

[114] I. Somerville, P. Vidaud, Surface spreading of charge due to ohmic conduction, Proceedings of the Royal Society A: Mathematical, Physical and Engineering Sciences 399 (1985) 277–293.

[115] O. Emelyanov, M. Shemet, Dielectric barrier discharge in needle-to-plane configuration: Model of surface charge relaxation, Journal of Electrostatics 81 (2016) 71–75. https://doi.org/10.1016/j.elstat.2016.04.001.

[116] H.T.M. Haenen, The characteristic decay with time of surface charges on dielectrics, Journal of Electrostatics 1 (1975) 173–185. https://doi.org/10.1016/0304-3886(75)90047-9.

[117] T.A. Yovcheva, G.A. Mekishev, A.T. Marinov, A percolation theory analysis of surface potential decay related to corona charged polypropylene (PP) electrets, Journal of Physics: Condensed Matter 16 (2004) 455.

[118] J.A. Geurst, Theory of Space-Charge-Limited Currents in Thin Semiconductor Layers, Phys. Stat. Sol. (b) 15 (1966) 107–118. https://doi.org/10.1002/pssb.19660150108.

[119] T.C. Chapman, H.J. Wintle, Surface-charge-limited transient currents on insulating surfaces, Journal of Applied Physics 53 (1982) 7425. https://doi.org/10.1063/1.330112.

[120] G. Sawa, J.H. Calderwood, Dependence of surface conduction current in oxidized polyethylene on electric field at various humidities, J. Phys. C: Solid State Phys. 4 (1971) 2313–2318. https://doi.org/10.1088/0022-3719/4/15/017.

[121] L. Zavattoni, C.-T. Vu, P. Vinson, A. Girodet, R. Hanna, O. Lesaint, Recommendations for surface conductivity characterisation under High Voltage Direct Current (HVDC), in: 2017 INSUCON - 13th International Electrical Insulation Conference (INSUCON), IEEE, Birmingham, United Kingdom, 2017: pp. 1–6. https://doi.org/10.23919/INSUCON.2017.8097176.

[122] B. Lutz, J. Kindersberger, Influence of relative humidity on surface charge decay on epoxy resin insulators, in: Properties and Applications of Dielectric Materials, 2009. ICPADM 2009. IEEE 9th International Conference on The, IEEE, 2009: pp. 883–886. http://ieeexplore.ieee.org/xpls/abs_all.jsp?arnumber=5252237 (accessed August 26, 2014).

[123] Y. Awakuni, J.H. Calderwood, Water vapour adsorption and surface conductivity in solids, Journal of Physics D: Applied Physics 5 (1972) 1038.

[124] S. Alam, Y. Serdyuk, S. Gubanski, Potential decay on silicone rubber surfaces affected by bulk and surface conductivities, IEEE Trans. Dielect. Electr. Insul. 22 (2015) 970–978. https://doi.org/10.1109/TDEI.2015.7076798.

[125] V.E. Shashoua, Static electricity in polymers. I. Theory and measurement, J. Polym. Sci. 33 (1958) 65–85. https://doi.org/10.1002/pol.1958.1203312608.

[126] V.E. Shashoua, Static electricity in polymers. II. Chemical structure and antistatic behavior, J. Polym. Sci. A Gen. Pap. 1 (1963) 169–187. https://doi.org/10.1002/pol.1963.100010114.

[127] X. Bai, A. Riet, S. Xu, D.J. Lacks, H. Wang, Experimental and Simulation Investigation of the Nanoscale Charge Diffusion Process on a Dielectric Surface: Effects of Relative Humidity, J. Phys. Chem. C 125 (2021) 11677–11686. https://doi.org/10.1021/acs.jpcc.1c02272.

[128] Ding Hai, Charge decay and transportation in teflon AF films, in: IEEE, 1994: pp. 89–94. https://doi.org/10.1109/ISE.1994.514749.

[129] P. Gunther, Mechanism of charge storage in electron-beam or corona-charged silicon-dioxide electrets, IEEE Trans. Elect. Insul. 26 (1991) 42–48. https://doi.org/10.1109/14.68225.

[130] P. Molinié, Considerations on diverse physical phenomena leading to return voltage on insulators, Journal of Electrostatics 115 (2022) 103674. https://doi.org/10.1016/j.elstat.2022.103674.

[131] N. Jonassen, How Fast Does a Charge Decay?, In Compliance 4 (2012) 18–21.